

# A Molecular Model for Lipid-Protein Interaction in Membranes: the Role of Hydrophobic Mismatch

Deborah R. Fattal and Avinoam Ben-Shaul

The Institute of Advanced Studies and The Fritz Haber Research Center for Molecular Dynamics, The Hebrew University of Jerusalem, Jerusalem 91904, Israel

**ABSTRACT** The interaction free energy between a hydrophobic, transmembrane, protein and the surrounding lipid environment is calculated based on a microscopic model for lipid organization. The protein is treated as a rigid hydrophobic solute of thickness  $d_p$ , embedded in a lipid bilayer of unperturbed thickness  $d_l^0$ . The lipid chains in the immediate vicinity of the protein are assumed to adjust their length to that of the protein (e.g., they are stretched when  $d_p > d_l^0$ ) in order to bridge over the lipid-protein hydrophobic mismatch ( $d_p - d_l^0$ ). The bilayer's hydrophobic thickness is assumed to decay exponentially to its asymptotic, unperturbed, value. The lipid deformation free energy is represented as a sum of chain (hydrophobic core) and interfacial (head-group region) contributions. The chain contribution is calculated using a detailed molecular theory of chain packing statistics, which allows the calculation of conformational properties and thermodynamic functions (in a mean-field approximation) of the lipid tails. The tails are treated as single chain amphiphiles, modeled using the rotational isomeric state scheme. The interfacial free energy is represented by a phenomenological expression, accounting for the opposing effects of head-group repulsions and hydrocarbon-water surface tension. The lipid deformation free energy  $\Delta F$  is calculated as a function of  $d_p - d_l^0$ . Most calculations are for  $C_{14}$  amphiphiles which, in the absence of a protein, pack at an average area per head-group  $a_0 \cong 32 \text{ \AA}^2$  ( $d_l^0 \cong 24.5 \text{ \AA}$ ), corresponding to the fluid state of the membrane. When  $d_p = d_l^0$ ,  $\Delta F > 0$  and is due entirely to the loss of conformational entropy experienced by the chains around the protein. When  $d_p > d_l^0$ , the interaction free energy is further increased due to the enhanced stretching of the tails. When  $d_p < d_l^0$ , chain flexibility (entropy) increases, but this contribution to  $\Delta F$  is overcounted by the increase in the interfacial free energy. Thus,  $\Delta F$  obtains a minimum at  $d_p - d_l^0 \cong 0$ . These qualitative interpretations are supported by detailed numerical calculations of the various contributions to the interaction free energy, and of chain conformational properties. The range of the perturbation of lipid order extends typically over few molecular diameters. A rather detailed comparison of our approach to other models is provided in the Discussion.

## 1. INTRODUCTION

Proper matching between the hydrophobic parts of membrane proteins and the surrounding lipid molecules is known to play a key role in controlling the biological activity of the proteins and the physicochemical properties of the lipid-protein matrix (Sackmann, 1984; Riegler and Möhwald, 1986; Peschke et al., 1987; Kurrle et al., 1990; Zhang et al., 1992; Abney and Owicki, 1985; Bloom et al., 1991; Mouritsen and Bloom, 1993). One familiar example is that of gramicidin-lipid membranes where the kinetics and thermodynamics of gramicidin dimerization (ion channel formation) is believed to depend sensitively on the "hydrophobic mismatch" between the thickness of the lipid bilayer's hydrophobic core and the hydrophobic length of the dimer (Hladky and Haydon, 1984; Elliott et al., 1983; Ring, 1992; Huang, 1986; Helfrich and Jakobsson, 1990). The basic notion here, as in various other systems, is that an integral protein tends to surround itself by lipids of matching size and shape. Since proteins are relatively rigid, whereas lipid hydrocarbon chains are flexible, the condition of hydrophobic matching can be fulfilled by stretching, squashing, and/or tilting of the lipid chains (Nezil and Bloom, 1992; Kurrle et al., 1990; Zhang et al., 1992). Similarly, in a mixed lipid

bilayer the presence of a hydrophobic protein can induce local segregation due to the protein's preference to be surrounded by appropriate lipids (Sackmann, 1984). All these phenomena involve structural changes in the lipid environment around the protein, which are reflected in various mechanical, conformational, and thermodynamic properties of the membrane (Bloom et al., 1991; Elliott et al., 1983; Sackmann, 1984; Jähnig et al., 1982; Peschke et al., 1987; Zhang et al., 1992). The effects of lipid-protein interactions are manifested, for example, in the degree of lipid chain order (Nezil and Bloom, 1992), in modified membrane (bending and stretching) elasticity (Ott et al., 1990), in variations in the bilayer's gel-fluid phase transition characteristics (Riegler and Möhwald, 1986; Peschke et al., 1987; Zhang et al., 1992; Kurrle et al., 1990) and, in some cases, in lipid-mediated protein aggregation (Pearson et al., 1983; Riegler and Möhwald, 1986).

The free energy cost associated with the incorporation of a protein, or any other hydrophobic solute, into the membrane, depends largely on the geometrical characteristics of the solute and on the molecular nature and composition of the unperturbed lipid bilayer. So far, only few theoretical studies have attempted to calculate the lipid-protein interaction free energy from a microscopic approach. (For detailed reviews, see Abney and Owicki (1985) and Mouritsen and Bloom (1993)). These include Marcelja's (1976) mean-field theory of chain packing in lipid-bilayers, which has been extended to a bilayer embedding a protein of the same hydrophobic

Received for publication 10 June 1993 and in final form 23 August 1993.

Address reprint requests to A. Ben-Shaul at the Fritz Haber Center.

© 1993 by the Biophysical Society

0006-3495/93/11/1795/15 \$2.00

thickness, as well as continuum theories based on the elastic theory of liquid crystals. In the latter, one calculates the elastic deformations of the lipid environment surrounding a protein whose hydrophobic thickness does not match that of the unperturbed lipid layer (Huang, 1986; Helfrich and Jakobsson, 1990). Very few computer simulation studies have been performed for specific systems, in order to calculate the changes in lipid conformational statistics resulting from the presence of a protein in the membrane (Edholm and Johansson, 1987; Scott and Cherng, 1978).

On the other hand, quite a few theoretical studies have addressed the effects of lipid-protein interactions on the gel-fluid transition of the bilayer (Caillé et al., 1980; Owicki and McConnell, 1979; Jähnig, 1981; Scott and Coe, 1983; Mouritsen and Bloom, 1984; Sperotto and Mouritsen, 1988). Most of these models are based on Landau-type expansions of the membrane free energy in terms of an "order parameter" measuring the protein-induced perturbation in lipid order. The (thermodynamic) order parameter can be the difference in the average orientational order parameter of the lipid acyl-chains between the perturbed and protein-free bilayer, the difference between the average area per chain in the two systems, or the hydrophobic mismatch between the protein and the unperturbed bilayer. From these models one can derive the functional form of, say, the deformation free energy, the shape of the hydrocarbon-water interface, and the shift in the phase transition temperature in terms of the lipid-bilayer thickness and protein dimensions. In general, these expressions involve some unknown phenomenological parameters.

The "mattress model" of Mouritsen, Bloom, and coworkers, is a phenomenological approach based on the theory of nonideal solutions, resembling in some respects the Landau theories mentioned above (Mouritsen and Bloom, 1984; Mouritsen and Bloom, 1993). In this model the free energy of the lipid-protein system is expressed as a sum of a mixing entropy term and a number of energy terms representing different contributions to the lipid-protein interaction energy. The latter include the direct van der Waals attraction between the solvent (lipid) and solute (protein), the excess "hydrophobic effect" associated with the lipid-protein hydrophobic mismatch, and the elastic deformation free energy of the lipid chains near the protein. The interaction potentials are estimated based on experimental data derived from thermodynamic and mechanical measurements of membrane properties. The mattress model has also been cast in a Monte Carlo (lattice) simulation scheme (Sperotto and Mouritsen, 1991) allowing for different microstates of the lipids, classified according to Pink's ten-state model (Pink and Chapman, 1979). This version of the model provides a connection between the microscopic characteristics of the system and its thermodynamic behavior.

Our major goal in this paper is to present a molecular theory, which accounts for the modifications in lipid conformational statistics attendant upon the addition of a protein to a lipid bilayer, and which enables a calculation of the lipid-protein interaction free energy as a function of the hy-

drophobic mismatch and other relevant molecular parameters. Among the outcomes of these calculations are estimates of the interaction parameters appearing in the phenomenological thermodynamic analyses of the lipid-protein system. Some of the calculated conformational properties, such as lipid-chain bond order parameter profiles, may be compared to measurable "single chain" properties.

The principal tool in our model is an extended version of a molecular (mean-field) theory for chain packing statistics in amphiphilic aggregates such as micelles or bilayers (Ben-Shaul et al., 1985) (for a recent review see Ben-Shaul and Gelbart (1993); for alternative mean-field/single-chain theories, see e.g. Gruen (1985) and Dill et al. (1988)). This theory has already been extensively applied to study a variety of issues pertaining to these systems, including, e.g., amphiphile organization and thermodynamics in mixed aggregates (Szleifer et al., 1987), inverted hexagonal phases (Steinhuizen et al., 1991) and surfactant monolayers, as well as stretching and bending elasticity of pure and mixed bilayers (Szleifer et al., 1990). In general, the predictions of the theory compare very well with available experimental and computer simulation studies. The basic quantity in this approach is the probability distribution of chain conformations, from which one can calculate any desired conformational or thermodynamic property. It is derived by minimizing the free energy of the system subject to molecular packing constraints and geometric boundary conditions. The resulting expressions for the probability distribution and the free energy involve a set of Lagrange parameters representing the lateral pressure profile across the hydrophobic core. These parameters are determined by solving the ("self-consistency") equations representing the packing constraints. The numerical procedure for evaluating the Lagrange parameters involves generation and classification of the accessible chain conformations. For amphiphiles with hydrocarbon chains comprising 18 segments or less, it is possible to enumerate all possible chain conformations. It should be noted that, for a given aggregation geometry (e.g., a planar bilayer of given thickness) the theory does not involve any adjustable parameters.

The major modification of the theory required for its application to the lipid-protein system is to account for the nonuniformity of the lipid local environment induced by the presence of the perturbing solute. As in previous applications of this theory (see, e.g., Ben-Shaul et al. (1985, 1993) and Szleifer et al. (1986, 1987, 1990) as well as in other theories of amphiphile chain packing (Dill et al., 1988; Gruen, 1985a, b)), we shall assume that the hydrophobic core of the membrane is liquid-like and thus characterized by a uniform density of lipid chain segments. This assumption, which is based on many experimental studies (see, e.g., Tanford, 1980; Israelachvili, 1985; Wennerström and Lindman, 1979) implies that the free energy cost corresponding to "hole formation" within the hydrophobic core is intolerably high (Gruen, 1985b). Based on this assumption, and after specifying the geometry of the hydrocarbon-water interface, one

can derive the probability distribution of chain conformations. Clearly, in the lipid protein system the conformational distribution function and any related property, such as the free energy per molecule, depend parametrically (in our case through the Lagrange parameters) on the distance from the protein. Following the phenomenological approaches mentioned above we shall assume (for systems with nonzero lipid-protein hydrophobic mismatch), that the hydrophobic thickness of the bilayer around the protein decays exponentially to its unperturbed, asymptotic, value (Owicki et al., 1978; Jähnig, 1981; Abney and Owicki, 1985). The “coherence length” characterizing the decay of the perturbation will be determined by minimizing the system’s free energy, which in addition to the lipid chain contribution includes a surface term accounting for the interactions in the interfacial (head-group) region. The latter will be modeled using a simple but rather general phenomenological representation.

## 2. MODEL

As in several previous models of lipid-protein interaction, we treat the hydrophobic part of a transmembrane protein as a rigid solute embedded in the bilayer’s hydrophobic core. The model presented below can be adapted to an arbitrary solute’s shape; the exact shape of the solute’s hydrophobic interface dictates the boundary conditions on the allowed chain conformations of the surrounding lipids. Clearly, different proteins are characterized by different interfacial shapes and different degrees of surface corrugation. Since our interest is focussed on the role of the hydrophobic mismatch, and in order to keep the discussion general, we shall assume that the protein’s interface can be treated as a smooth hydrophobic wall. For the sake of concreteness we may suppose that the protein is a cylinder of diameter  $D$  and height  $d_p$ , symmetrically situated with respect to the bilayer’s midplane. We further assume that  $D \gg a^{1/2}$ , where  $a$  is the average cross-sectional area per lipid molecule in the bilayer, i.e., the average area per head-group at the hydrocarbon-water interface. This assumption implies that, to the lipid molecules in its vicinity, the protein appears as a (nearly) planar hydrophobic wall. The assumption of a planar wall is made only for computational convenience; the curvature of the impenetrable protein’s wall enters only through the boundary conditions on the allowed conformations of the lipid chains in the immediate vicinity of the protein (see Appendix). (For  $D \gg a^{1/2}$  the effects of the protein’s (cross-sectional) curvature on the conformational and thermodynamic properties of the surrounding lipid molecules are negligible.)

We choose an arbitrary point on the line where the bilayer’s midplane meets the protein wall as the origin of a cartesian coordinate system, with the  $z$ -axis perpendicular to the bilayer’s plane  $xy$ . The protein wall is parallel to the  $yz$  plane, at  $x = 0$ ; see Fig. 1.

Let  $d_L(x)$  denote the thickness of the hydrophobic core at distance  $x$  from the protein, i.e.,  $z = d_L(x)/2$  and  $z = -d_L(x)/2$  are, respectively, the distances of the “upper” and “lower” hydrocarbon-water interfaces from the membrane midplane.

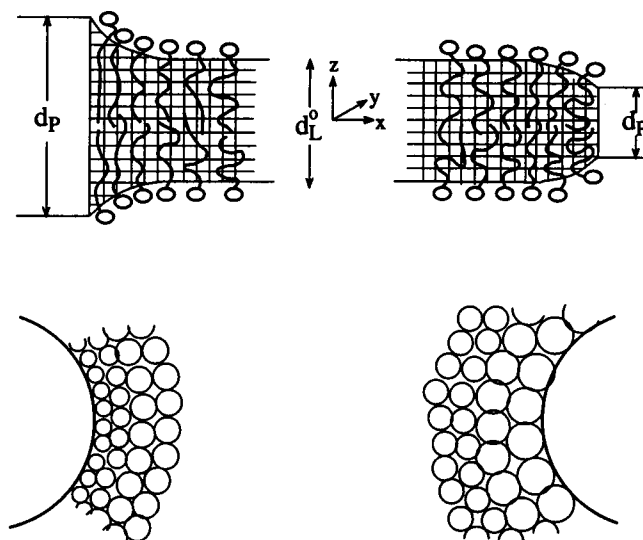


FIGURE 1 Schematic illustration of the model and the relevant molecular parameters. Top: a two-dimensional “side view” of chain packing around the protein; positive hydrophobic mismatch (*left*), negative mismatch (*right*). Bottom: “top view,” illustrating the radial variation in chain cross-sectional area around the protein.

Following some of the phenomenological (Landau-type) theories of lipid-protein interactions (Owicki et al., 1978; Jähnig, 1981; Abney and Owicki, 1985), we assume

$$d_L(x) = d_L^0 + (d_p - d_L^0) \exp(-x/\xi), \quad (1)$$

where  $d_L^0 = d_L(x = \infty)$  is the hydrophobic thickness of the unperturbed (protein-free) bilayer and  $\xi$  is the “coherence length” of the perturbation. We shall treat  $\xi$  as a variational parameter, to be determined by minimization of the bilayer deformation free energy  $\Delta F$  (see below). It should be noted that the exponential thickness profile, Eq. 1, is not a consequence of the molecular theory of chain packing presented and analyzed below. Rather, it is a convenient single-parameter representation of  $d_L(x)$ . Of course, more general  $d_L(x)$  profiles could be tested, but at the cost of introducing additional variational parameters.

The deformation free energy is largely due to the fact that the lipid chains must be stretched (when  $d_p - d_L^0 > 0$ ) or compressed (when  $d_p - d_L^0 < 0$ ) in order to satisfy the hydrophobic matching condition  $d_L(x = 0) = d_p$ , implied by Eq. 1; see Fig. 1. These elastic contributions to  $\Delta F$  are partly counter-balanced by surface tension terms accounting for the corresponding changes in the average interfacial area per molecule when  $d_p \neq d_L^0$ . Note, however, that  $\Delta F > 0$  even when  $d_L^0 = d_p$ , because of the restricted conformational freedom of the lipid chains neighboring the protein wall.

The central quantity in the forthcoming discussion is the probability distribution of chain conformations  $P(\alpha; x)$  of lipid chains anchored at distance  $x$  from the protein;  $\alpha$  denoting a given chain conformation (Eq. 8 below).  $P(\alpha; x)$  determines both single-chain conformational properties, such as bond orientational order parameters (Eq. 14 below) and thermodynamic properties, such as the chain conforma-

tional free energy (Eqs. 5 and 9). The derivation of the functional form of  $P(\alpha; x)$  does not depend on the special characteristics of the chain (e.g., its length or the number and position of double bonds along the chain). These details enter only in the specific calculations of the molecular parameters appearing in  $P(\alpha; x)$  (the Lagrange multipliers,  $\lambda(S)$ , see Eq. 8). Thus, the theory can be applied to various chain models, as well as to lipid mixtures (see, e.g., Szleifer et al., 1987; Ben-Shaul and Gelbart, 1993). However, in the calculations presented in Results and Analysis we shall consider bilayers composed of simple, single tail, amphiphiles of the type  $P-(\text{CH}_2)_{n-1}-\text{CH}_3$  with  $P$  symbolizing the polar head-group. (Alternatively, the bilayer may be regarded as composed of double-chain lipids,  $P'-[(\text{CH}_2)_{n-1}-\text{CH}_3]_2$ , provided the interactions between chains originating from the same head-group are no different from those belonging to different neighboring lipids.) Thus, in the derivation below we shall generally refer to the conformations,  $\alpha$ , of simple (saturated) acyl chains,  $-(\text{CH}_2)_{n-1}-\text{CH}_3$ .

Assuming, as usual, that the hydrophobic core is liquid-like, the effective volume occupied by a single alkyl tail in the core is  $v \equiv (n-1)m + m'$  where  $m \approx 27 \text{ \AA}^3$  and  $m' \approx 2m$  are, respectively, the common estimates for the specific volumes of  $\text{CH}_2$  and  $\text{CH}_3$  segments in bulk liquid alkanes (Tanford, 1980; Israelachvili, 1985). Similar values were found for the segment volumes of acyl chains in the fluid state of lipid bilayers (see, e.g., Nagle and Wilkinson, 1978; Wilkinson and Nagle, 1981; Lewis and Engelman, 1983; Nagle and Wiener, 1988; Wiener and White, 1992). Yet, it should be noted that other values have also been proposed (Small, 1986). It should be stressed that the specific volumes,  $m$  and  $m'$ , enter the calculations only indirectly, through the conversion,  $a(x) = v/[d_L(x)/2]$  (see below), from the bilayer thickness ( $x$ ) to the average cross sectional area per chain,  $a(x)$ . The quantity entering directly into the calculations (as a geometric boundary condition) is the bilayer's thickness  $d_L(x)$  (see Appendix and the discussion following Eq. 5 below). The relevant molecular parameters for the characterization of different chain conformations are the C—C bond lengths and the C—C—C bond angles, according to the rotational isomeric state model (see below). Note also that the length,  $l$ , of a fully extended ("all-trans")  $P-(\text{CH}_2)_{n-1}-\text{CH}_3$  chain, from  $P$  to the terminal  $\text{CH}_3$ , is  $l \approx 1.27 \text{ n\AA}$  (Flory, 1969). Clearly,  $d_L(x)/2 \leq l$ .

Eq. 1, which describes the shape of the hydrocarbon-water interface, also determines the two-dimensional density of lipid chains (or head-groups) in the membrane. More specifically, let  $\sigma(x, y)\delta x\delta y$  denote the number of head-groups, anchored to the interface of the upper leaflet, whose projections on the bilayer's midplane fall within the small area element  $\delta x\delta y$  around  $x, y$ . Similarly, we use  $\sigma'(x, y)$  to denote the two-dimensional density of the head-groups in the lower monolayer. Since our system is translationally invariant along the  $y$  direction, it follows that  $\sigma = \sigma(x)$ .  $1/\sigma(x, y) = 1/\sigma(x)$  is the average cross-sectional area per lipid chain in the  $xy$  plane. From the assumption that the hydrophobic core is liquid-like it follows that

$\sigma(x) = d_L(x)/2v$ . At a large distance from the protein  $d_L(x) \rightarrow d_L^0$  and  $\sigma(x) \rightarrow d_L^0/2v = 1/a_0$ , where  $a_0 = a(x = \infty)$  is the unperturbed area per head-group. Note, however, that whenever the interface is curved (i.e., when  $d_L(x) \neq d_L^0$ ) then  $\sigma(x) \neq 1/a(x)$ , where  $a(x)$  is the local area per head-group (see below).

Let  $f(x, y)$  denote the free energy per molecule, for those molecules in the upper monolayer whose head-group coordinates  $x_h, y_h$  fall within  $\delta x\delta y$  around  $x, y$ . The  $z$  coordinate of the head-group is determined by (1),  $z_h = z_h(x) = d_L(x)/2 \pm \delta z$ , where  $\delta z \ll d_L(x)$  defines a narrow interfacial shell confining the head-group. (In the numerical calculations we allow the first two chain segments to protrude, occasionally, into the interfacial shell; see below).

The symmetry of the system implies that  $f = f(x)$  is independent of  $y$ . Using  $f' = f'(x)$  to denote the local free energy per molecule in the lower monolayer, the bilayer free energy (per unit length along the  $y$  direction) is given by

$$F = \int dx [\sigma(x)f(x) + \sigma'(x)f'(x)] \quad (2a)$$

$$= 2 \int dx \sigma(x)f(x), \quad (2b)$$

with the second equality holding for symmetrical bilayers. The integration over  $x$  extends from 0 to some arbitrary distance  $L \gg \xi$ , where the lipid perturbation is negligible.  $N = 2 \int \sigma(x) dx$  is the number of molecules (per unit length along  $y$ ) between  $x = 0$  and  $L$ . The lipid-protein interaction free energy is given by  $\Delta F = F - F^0$  with  $F^0 = Nf_0$  denoting the free energy of the unperturbed (protein-free) bilayer.  $f_0 = f(x \rightarrow \infty)$  is the free energy per molecule in the unperturbed system. It should be stressed that neither Eq. 2a nor Eq. 2b imply that the bilayer is a sum of two independent monolayers. That is, chains from one monolayer can cross the midplane (interdigitate) into the other monolayer.

To a very good approximation  $f(x)$ , and hence  $F$ , can be expressed as a sum of "tail" and "head-group" contributions (Ben-Shaul and Gelbart, 1993)

$$f(x) = f_t(x) + f_h(x). \quad (3)$$

The first term accounts for the conformational free energy of the amphiphile's hydrocarbon chain which depends, rather sensitively, on the local packing geometry; i.e., on  $\sigma(x)$  and  $a(x)$ .  $f$  also includes the cohesive (van der Waals attraction) energy of the hydrocarbon tails which, based on the assumption of uniform density within the hydrophobic core, can be treated as a constant. The second term in Eq. 3 includes the interactions prevailing in the interfacial region, i.e., those between neighboring head-groups, and between the surface of the hydrophobic core and the surrounding aqueous solution.

Consider first the hydrocarbon-core (tails') contribution to the free energy, which will be calculated based on the mean-field theory of amphiphile chain packing mentioned in section 1. According to this approach

$$F_i = \int dx \left\{ \sigma(x) \sum_{\alpha} P(\alpha; x) [\epsilon(\alpha) + kT \ln P(\alpha; x)] + \sigma'(x) \sum_{\alpha'} P'(\alpha'; x) [\epsilon(\alpha') + kT \ln P'(\alpha'; x)] \right\}, \quad (4)$$

with the first and second sums representing the local free energy per molecule in the upper and lower monolayer, respectively. Explicitly,

$$f_i(x) = \sum_{\alpha} P(\alpha; x) \epsilon(\alpha) + kT \sum_{\alpha} P(\alpha; x) \ln P(\alpha; x) \quad (5a)$$

$$= \epsilon_i(x) - Ts_i(x), \quad (5b)$$

is the local chain free energy in the upper monolayer. In Eqs. 4 and 5,  $\epsilon(\alpha)$  is the internal (*trans/gauche*) energy of a chain in conformation  $\alpha$ .  $P(\alpha; x)$  is the local singlet probability distribution function (*pdf*) of chain conformations, corresponding to chains originating from the upper interface, at distance  $x = x_h$  from the protein.  $\epsilon_i(x)$  and  $s_i(x)$  are the local energy and entropy per chain.

In our calculations a given chain conformation  $\alpha$  is fully specified by  $\alpha = b, z_h, \Omega$ , as follows:  $b$  is the *trans/gauche* sequence of the skeletal atoms of the lipid  $P-(CH_2)_{n-1}-CH_3$ , characterized in terms of the rotational isomeric state (RIS) model (Flory, 1969). The head-group  $P$  may be regarded as the "zeroth chain segment." (The number of possible bond sequences is  $3^{n-1}$ , including non-self-avoiding conformations which are discarded from the calculations). The internal energy is  $\epsilon(\alpha) = \epsilon(b) = n_g(b)\epsilon_g$  where  $n_g(b)$  is the number of *gauche* bonds of a chain with bond sequence  $b$ .  $\epsilon_g = 500$  cal/mole is the *gauche* energy (Flory, 1969) used in the calculations.  $z_h$  is the  $z$  coordinate of the head-group, i.e., its position with respect to the midplane;  $\Omega$  denotes the overall orientation of a chain (with a fixed bond sequence), with respect to the interface, as specified by three Euler angles.

An explicit expression for  $P(\alpha; x)$  can now be derived by seeking the particular *pdf* which minimizes  $F_i$  subject to whichever constraints  $P(\alpha; x)$  must fulfill. Apart from the trivial normalization condition,  $\sum_{\alpha} P(\alpha; x) = 1$ , the only relevant constraints on  $P(\alpha; x)$  are those implied by the requirement for uniform chain segment density inside the hydrophobic core. To formulate this constraint mathematically, let  $\mathbf{R}$  denote a point inside the hydrophobic core. Now consider a chain in conformation  $\alpha$  originating from a point  $\mathbf{r} = x, y, z$  on the upper interface. (Recall that  $z = z_h$  is included in the definition of  $\alpha$ .) For this chain we use  $\phi(\mathbf{R}, \alpha; x, y) d\mathbf{R}$  to denote the number of chain segments ( $CH_2$  groups) within the volume element  $d\mathbf{R}$  around point  $\mathbf{R}$ . ( $CH_3$  groups count as two segments since  $m'(CH_3) \approx 2 m(CH_2)$ ). Similarly, we use  $\phi'(\mathbf{R}, \alpha'; x, y)$  to denote the segment density at  $\mathbf{R}$  due to chains originating at the lower interface. Using  $\rho(\mathbf{R})$  to denote the local segment density

at  $\mathbf{R} = X, Y, Z$  we obtain

$$\rho(\mathbf{R}) = \int dx dy \left\{ \sigma(x) \sum_{\alpha} P(\alpha; x) \phi(\mathbf{R}, \alpha; x, y) + \sigma'(x) \sum_{\alpha'} P'(\alpha'; x) \phi'(\mathbf{R}, \alpha'; x, y) \right\} = \rho = \text{constant}. \quad (6)$$

The first equality is general, with the two terms accounting for the contributions to  $\rho(\mathbf{R})$  from chains hanging on opposite interfaces. The second equality expresses the requirement for uniform density throughout the hydrophobic core. (Liquid-like density corresponds to  $\rho = 1/m$ .)

The symmetry of our system implies that  $\rho(\mathbf{R})$  is independent of  $Y$ , even if  $\rho(\mathbf{R})$  is not constant. Similarly,  $\int dy \phi(\mathbf{R}, \alpha; x, y) \equiv \psi(X, Z, \alpha; x) \equiv \psi(S, \alpha; x)$  is independent of  $Y$ , with  $S \equiv X, Z$  (see Fig. 1). By definition,  $\psi(X, Z, \alpha; x) \delta X \delta Z$  is the number of segments of a chain in conformation  $\alpha$ , originating at  $x$ , which fall within  $\delta X \delta Z$  irrespective of their  $Y$  coordinate. Thus, Eq. 6 can be rewritten as

$$\int dx \left\{ \sigma(x) \sum_{\alpha} P(\alpha; x) \psi(S, \alpha; x) + \sigma(x) \sum_{\alpha'} P(\alpha'; x) \psi'(S, \alpha'; x) \right\} = \rho, \quad (7)$$

for all  $S$  within the hydrophobic core. Note that  $\rho(S)$  involves contributions from any chain, from either monolayer, which can reach  $S$ . Clearly, the main contribution to  $\rho(X, Z)$  in, say, the upper monolayer ( $Z > 0$ ) arises from chains with head-group coordinates  $x \sim X$  and  $z \sim d_L(x)/2$ .

The functional minimization of Eq. 4 with respect to  $\{P(\alpha; x)\}$ , subject to Eq. 7, yields

$$P(\alpha; x) = \frac{1}{q(x)} \exp \left[ -\beta \epsilon(\alpha) - \beta \int dS \lambda(S) \psi(S, \alpha; x) \right], \quad (8)$$

where  $\beta = 1/kT$ . The normalization factor,  $q(x)$ , is a local isothermal-isobaric partition function; i.e.,  $g_i(x) = -kT \ln q(x)$  is the local free energy per chain. The  $\lambda(S)$  are the Lagrange multipliers conjugate to the uniform density constraint Eq. 7. Their values are determined by substituting Eq. 8 into Eq. 7 and solving, for all  $S$ , the resulting (self-consistency) equations. The  $\lambda(S)$  depend on the bilayer's geometry, which in our case is dictated by  $\{\sigma(x)\}$  or, equivalently, by  $\{d_L(x)\}$ . Once the  $\lambda(S)$  and hence  $P(\alpha; x)$  are known, we can use Eq. 8 to calculate any chain conformational property of interest, e.g., the bond order parameter profile of the chains. Thermodynamic properties can also be calculated. In particular,  $F_i$  is obtained by substituting Eq. 8 into Eq. 4. Note also that using Eq. 7 we find that this substitution yields (for

a symmetric bilayer)

$$F_t = -2kT \int dx \sigma(x) \ln q(x) - \rho \int dS \lambda(S). \quad (9)$$

The first term here is  $G_t$ , the Gibbs free energy of the tails (per unit protein length), and the second term is a generalized "PV" contribution.

Equation 9 reduces to a simpler form for the protein-free (planar) bilayer. In this case the system is translationally invariant along the  $x$  direction, so that  $q(x) = q$ ,  $\lambda(S) = \lambda(X, Z) = \lambda(Z) = \lambda(-Z)$ , and  $\sigma(x) = 1/a_0$  where  $a_0$  is the unperturbed head-group area. Performing the  $x$  and  $X$  integrations in Eq. 9 between 0 and  $L$ , and noting that the free energy per molecule is given by  $f_t^\circ = a_0 F_t^\circ / 2L$ , we obtain

$$f_t^\circ = -kT \ln q - a_0 \rho \int_0^{a_0/2} dZ \lambda(Z). \quad (10)$$

Here,  $\rho \lambda(Z) dZ \equiv \pi(Z) dZ$  is the lateral pressure in the thin shell  $Z, Z + dZ$  of the hydrophobic core.

For the planar, unperturbed, bilayer the self-consistency equations Eq. 7 reduce to a set of coupled nonlinear equations which can easily be solved numerically for the  $\lambda(Z)$ , for arbitrary head-group areas  $a$ . For the lipid-protein membrane the numerical procedure for evaluating the  $\lambda(S)$  is somewhat more involved, but still straightforward, as outlined in the next section and the Appendix.

The tightly packed hydrocarbon chains in the hydrophobic core are generally stretched beyond their optimal length and thus tend to contract in order to restore their conformational freedom. This leads to a lateral, interchain, repulsive pressure  $\pi_t = -\partial f_t / \partial a > 0$  which tends to increase the average area per chain,  $a$ . The rapid decrease of  $f_t(a)$  (at small values of  $a$ ), as revealed by Fig. 2, demonstrates this behavior for  $C_{12}$ ,  $C_{14}$ , and  $C_{16}$  chains packed in a planar, unperturbed bilayer.  $f_t$  obtains a minimum at  $a = a_t$  ( $\sim 40$ – $45 \text{ \AA}^2$  for  $C_{14}$ – $C_{16}$  chains), corresponding to an average end-to-end chain length  $l = l_t = \nu/a_t$ . The slow increase of  $f_t(a)$  beyond  $a_t$  is due to chain compression ( $l < l_t$ ).

The optimal area per chain in bilayers,  $a_0$ , is generally considerably smaller than  $a_t$ . Since, by definition,  $a_0$  is determined by the equilibrium (minimum) condition  $\partial(f_h + f_t)/\partial a = 0$ , it follows that interchain repulsion is counterbalanced by a net attractive pressure (surface tension)  $\pi_h = -\partial f_h / \partial a < 0$  operating in the head-group region.

The interfacial free energy,  $f_h$ , is generally a complicated function of  $a$  and the interfacial curvature, depending on the specific nature of the head-groups and the ambient aqueous solution (see, for example, Dill and Stigter (1988), Stigter and Dill (1988), Winterhalter and Helfrich (1992), Ennis (1992), and Andelman (1994)). We shall therefore adopt here an approximate, but quite general, phenomenological representation of  $f_h$  in terms of the "opposing forces" (Israelachvili, 1985; Tanford, 1980; Israelachvili et al., 1976). In this representation  $f_h(a) = \gamma a + c/a = 2\gamma a_h + \gamma a(1 - a_h/a)^2$  is a sum of an attractive and a repulsive term

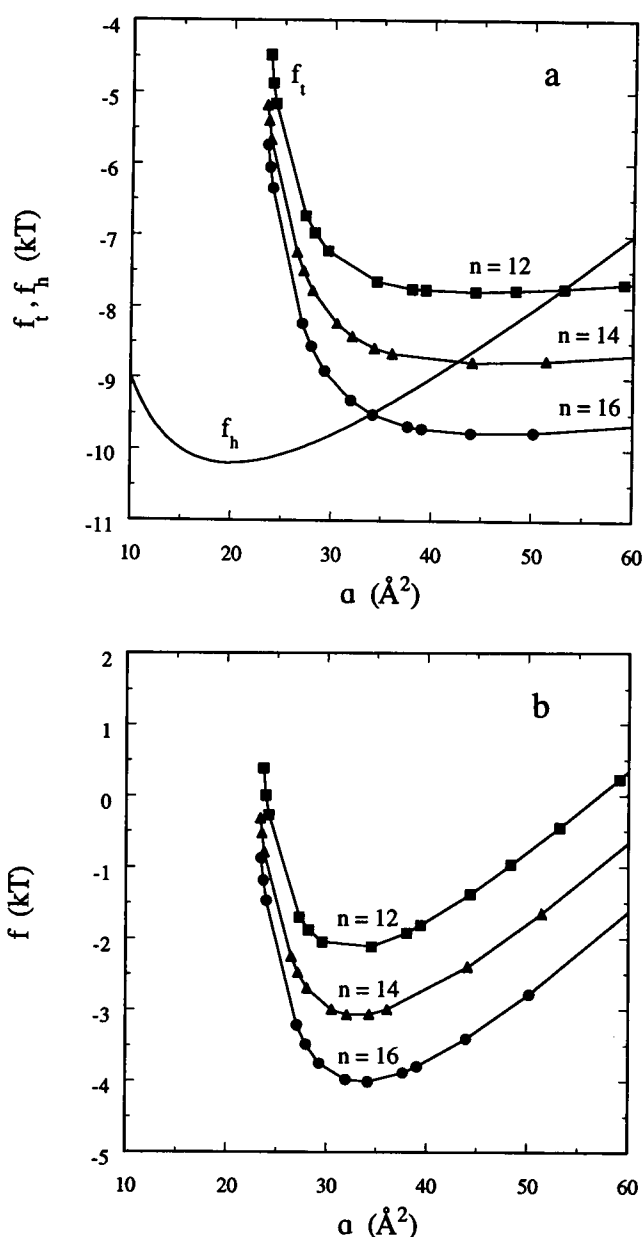


FIGURE 2 (a) Head ( $f_h$ ) and tail ( $f_t$ ) contributions to the free energy per molecule,  $f$ , as a function of the area per head-group, for a protein-free bilayer composed of single chain amphiphiles of chain length  $n = 12$  (■), 14 (▲), and 16 (●). The chain free energies are measured, for each  $n$ , relative to the all-*trans* conformation (where both the energy and entropy per chain are set equal to zero).  $f_h$  (solid line) is calculated using Eq. 12, with  $a_h = 20 \text{ \AA}^2$  and  $\gamma = 0.12 \text{ kT/\AA}^2$  ( $T = 300\text{K}$ ), relative scale. (b) The sum of tail and head free energies for the chains shown in a.

accounting, respectively, for the surface free energy ( $\gamma a$ ) associated with the exposure of the hydrocarbon core to the surrounding aqueous solution, and for the repulsion, electrostatic and/or excluded volume, ( $C/a$ ), between the head-groups.  $\gamma$ , which can be interpreted as an effective surface tension is usually estimated as  $\gamma \approx 50 \text{ erg/cm}^2 \approx 0.12 \text{ kT/\AA}^2$  at room temperature (Israelachvili et al., 1976; Israelachvili, 1985).  $C$  measures the strength of head-group repulsion and  $a_h = (C/\gamma)^{1/2}$  is the value of  $a$  for which  $f_h$  is minimal.

Clearly,  $a_h < a_0 < a_t$ . Before discussing the choice of numerical values for  $\gamma$  and  $C$  (equivalently  $\gamma$  and  $a_h$ ), let us first write  $f_h$  for the lipid-protein bilayer.

The extension of the above scheme to the deformed bilayer is straightforward. Namely, we write

$$f_h(x) = \gamma a(x) + C/a(x) \quad (11)$$

$$= 2\gamma a_h + \gamma a(x)[1 - a_h/a(x)]^2, \quad (12)$$

where  $a(x)$  is the local interfacial area per molecule, at distance  $x$  from the protein.  $a(x)$  is related to the interface profile  $d_L(x)$ , as follows. Consider a "slice" of the bilayer, of length  $B$  along the  $y$ -axis (i.e., parallel to the protein's plane) and width  $\delta x$  along  $x$ . The number of chains in this region is  $\delta N(x) = 2B\sigma(x)\delta x = Bd_L(x)\delta x/v$ , where  $v$  is the chain's volume. The interfacial area of the above slice (in both monolayers) is  $2\delta A(x) = 2B\delta x[1 + (d'_L(x)/2)^2]^{1/2}$ , with  $d'_L(x) = d[d_L(x)]/dx$ . Thus,  $a(x) = 2\delta A(x)/\delta N(x)$  is given by

$$a(x) = 2v/d_L(x)\{1 + [d'_L(x)/2]^2\}^{1/2}. \quad (13)$$

The planar bilayer limit corresponds to  $a(x \rightarrow \infty) = a_0 = 2v/d_L^0$ .

The optimal area per head-group  $a_0$  will be treated as an experimental "input parameter" in our calculations; e.g., for  $C_{14}$  chains we shall take  $a_0 = 32 \text{ \AA}^2$ , corresponding to the typical value of  $\sim 60\text{--}65 \text{ \AA}^2$  found for the area per head-group of many double-chain phospholipids (see, for example, Lewis and Engelman, 1983). Recall that  $a = a_0$  is the solution of  $\pi_t(a) + \pi_h(a) = 0$  for the unperturbed bilayer, with  $\pi_t = -\partial f_t/\partial a$  and  $\pi_h = -\partial f_h/\partial a = -\gamma + C/a^2 = -\gamma[1 - (a_h/a)^2]$ , cf. Eq. 13. Since, for a given chain length, there are no free parameters in our calculation of  $f_i(a)$ , only certain combinations of the parameters  $\gamma$  and  $a_h$  will be consistent with the specified value of  $a_0$ . In other words,  $\gamma$  and  $a_h$  are not independent parameters. For instance, if we take the commonly accepted value  $\gamma = 0.12 \text{ kT/\AA}^2$ , then for  $C_{14}$  chains with  $a_0 \approx 32 \text{ \AA}^2$  we find  $a_h \approx 20 \text{ \AA}^2$  (corresponding to  $\approx 40 \text{ \AA}^2$  for a double chain amphiphile) (Fig. 2 a). Note that in this case head-group repulsion,  $\gamma(a_h/a_0)^2 \sim 0.4\gamma$  is weaker than chain repulsion. (More precisely, head-group repulsion is shorter ranged.) Smaller values of  $\gamma$  imply smaller  $a_h$ , e.g., for  $\gamma \approx 0.08 \text{ kT/\AA}^2$ , we find that in order to obtain  $a_0 \approx 32 \text{ \AA}^2$  we must set  $a_h \approx 0$ . It should be noted however that  $a_0$  is not very sensitive to small variations in  $\gamma$  and  $a_h$ . For instance, for  $\gamma = 0.12 \text{ kT/\AA}^2$  variations of  $a_h$  between 0 and  $20 \text{ \AA}^2$  change  $a_0$  by less than  $2 \text{ \AA}^2$ . Thus, in the calculations of  $\Delta F$  presented in the next section we shall consider several  $\gamma, a_h$  combinations.

We close this section with a remark on the chain length dependence of  $a_0$ . Our calculations show that  $a_0$  increases very slowly with  $n$ , Fig. 2 b. This behavior can be explained qualitatively based on an approximate scaling argument, as follows. Let  $l_t$  denote the average end-to-end distance of a conformationally disordered chain (i.e.,  $l_t = v/a_t$  with  $a_t$  corresponding to minimal  $f_t$ ). For these, "ideal," chains (as in polymer melts),  $l_t \sim n^{1/2}$ . The free energy cost associated with stretching the chain to length  $\bar{l} = d_L/2 = v/a$  (in the

Gaussian approximation),  $f_t \sim (\bar{l}/l_t)^2 \sim (v/an^{1/2})^2$ . Since  $v \sim n$  we find  $f_t \sim n/a^2$ . Now suppose for simplicity that  $f_h = \gamma a$  (i.e., we ignore head-group repulsion). Minimization of  $f = f_t + f_h = \kappa n/a^2 + \gamma a$  ( $\kappa = \text{constant}$ ) now yields  $a_0 \sim n^{1/3}$ , hence  $\bar{l} \sim n^{1/3}$ , which explains the slow increase of  $a_0$  with  $n$ . It should be noted that inclusion of head-group repulsion implies an even weaker dependence of  $a_0$  on  $n$ . (Obviously,  $a_0$  would be totally independent of  $n$  if chain repulsion is negligible compared to head-group repulsion, in which case  $a_0 = a_h$ .) The weak dependence of  $a_0$  or, equivalently, the bilayer thickness  $d_L^0 = 2v/a_0$ , on  $n$  is consistent with experiment (Israelachvili, 1985; Lewis and Engelman, 1983).

### 3. RESULTS AND ANALYSIS

All the results presented in this section are for bilayers composed of  $P\text{-(CH}_2\text{)}_{13}\text{-CH}_3$  (" $C_{14}$ ") lipids. The interfacial, head-group, interactions were modeled using Eqs. 12 and 13 and the chain packing statistics was treated according to Eqs. 4–9. Several cases of lipid-protein hydrophobic mismatch have been analyzed, ranging from  $(d_p - d_L^0)/2 = -3.5$  to  $+3.5 \text{ \AA}$ . In all cases the unperturbed hydrophobic thickness of the bilayer is  $d_L^0 = 24.5 \text{ \AA}$ , corresponding to an average area per lipid head-group  $a_0 = d_L^0/2v \approx 32 \text{ \AA}^2$ . The hydrophobic region profile is assumed to be of the form of Eq. 1, with  $\xi$  treated as a variational parameter. Namely, for every hydrophobic mismatch  $d_p - d_L^0$ , the deformation free energy  $\Delta F = F - F_0$  was calculated for different  $\xi$  values and the optimal  $\xi$  was chosen as that which minimizes  $\Delta F$ . The main numerical effort in the calculations involves the evaluation of the *pdfs* of chain conformations  $P(\alpha; x)$ . The numerical procedure for the evaluation of the conformational *pdf* is outlined in the Appendix. In the discussion below we first analyze the effects of the protein's hydrophobic wall on the conformational properties of nearby lipid chains, and then consider the combined effects of chain and head-group interactions on the lipid-protein deformation free energy.

All the calculations reported below have been performed for a constant temperature,  $T = 300\text{K}$ , assuming that at this temperature the bilayer is in its fluid ("liquid-crystalline") state. Previous calculations have shown (Szleifer et al., 1986) that in this state, the conformational properties of the lipid chains (e.g., bond order parameter profiles and spatial distributions of chain segments) are governed, primarily, by the packing constraints, i.e., by interchain excluded volume interactions, whereas internal energy effects play only a secondary role. More explicitly, by varying the *gauche* energy  $\epsilon_g$  (which enters into the calculation through  $\epsilon(\alpha)/kT$  in Eq. 8), it was found that, for a given value of the head-group area  $a$ , the conformational properties derived from  $P(\alpha)$  are rather insensitive to  $\epsilon_g/kT$ . Clearly, however, temperature variations play a crucial role near the liquid-crystalline–gel transition of the bilayer, which is not considered in this paper.

## a) Chain conformational properties

Many of the conformations available to the lipid chains in an unperturbed membrane are not accessible for the chains in the vicinity of the protein. The excluded conformations are those which, had the protein not been there, would penetrate into the protein region,  $x < 0$  in Fig. 1. Thus, the presence of the impenetrable protein wall results in a loss of lipid chain conformational entropy  $\Delta s_i(x) = s_i(x) - s_i^0 < 0$  which decreases as the distance of the head-group from the protein,  $x$ , increases, ( $s_i^0 = s_i(x \rightarrow \infty)$ ). This effect exists, although to different extents, for positive, negative and zero hydrophobic mismatches,  $d_p - d_L^0$ , as demonstrated in Fig. 3. The special case  $d_p - d_L^0 = 0$  is the one originally considered by Marcelja (1976).

Fig. 3 shows the energetic and entropic contributions to the excess lipid chain conformational free energy  $\Delta f_i = f_i(x) - f_i^0 = \Delta \epsilon_i - T\Delta s_i$ , as a function  $x$ , for three values of  $d_p - d_L^0$ . The values of the coherence length,  $\xi \approx 6 \text{ \AA}$  for  $(d_p - d_L^0)/2 = -3.5 \text{ \AA}$  and  $\xi \approx 3 \text{ \AA}$  for  $(d_p - d_L^0)/2 = 3.5 \text{ \AA}$ , correspond to the minimal deformation free energy  $\Delta F = \Delta F_i + \Delta F_h$  for  $\Delta F_h$  modeled using  $\gamma = 0.12 \text{ kT/\AA}^2$  and  $a_h = 20 \text{ \AA}^2$  (see section 2 and section 3b below). Note that the range of the deformation is  $\sim 3\xi$ . The results reveal that the entropic term  $-T\Delta s_i$  is the major contribution to  $\Delta f_i$ , reflecting significant loss of conformational freedom. On the other hand,  $\Delta \epsilon_i$  is relatively small, indicating a small change in the average fraction of *gauche* conformers.

The deformation free energy in the case of zero hydrophobic mismatch,  $d_p - d_L^0 = 0$ , is due entirely to the presence of the rigid protein wall, which tends to align the chains in its immediate vicinity. This boundary condition disfavors chain conformations with a large number of *gauche* bonds, as reflected by the (small) negative value of  $\Delta \epsilon_i$  for low  $x$ , Fig. 3 a. When  $d_p > d_L^0$  the lipid chains must stretch out in order to satisfy the hydrophobic matching condition  $d_p = d_L(x = 0)$ . This leads to additional loss of conformational entropy (as compared to the case  $d_p = d_L^0$ ), and a somewhat lower chain energy due to the enhanced statistical weight of conformations with low *gauche* content, Fig. 3 b. On the other hand, when  $d_p < d_L^0$  the average cross-sectional area per chain is relatively large ( $a(x) \sim d_L(x)/2\nu > a_0 = d_L^0/2\nu$ ), allowing for more conformational freedom which partly compensates for the loss of conformations implied by the protein wall. In this case,  $\Delta \epsilon_i$  is positive (yet small), due to the higher probability of *gauche* conformers.

The above notions are supported by calculations of other conformational properties of the lipid chains. In Fig. 4 we show calculated C—H bond order parameter profiles (Edholm, 1982; Bloom et al., 1991) for the same three cases considered in Fig. 3. More explicitly,

$$S_k(x) = \langle (3 \cos^2 \theta_k - 1)/2 \rangle$$

$$= \sum_{\alpha} P(\alpha; x) [3 \cos^2 \theta_k(\alpha; x) - 1]/2, \quad (14)$$

where  $\theta_k(\alpha; x)$  is the angle between the membrane normal and the  $C_k$ —H bond of a lipid chain in conformation  $\alpha$ ,

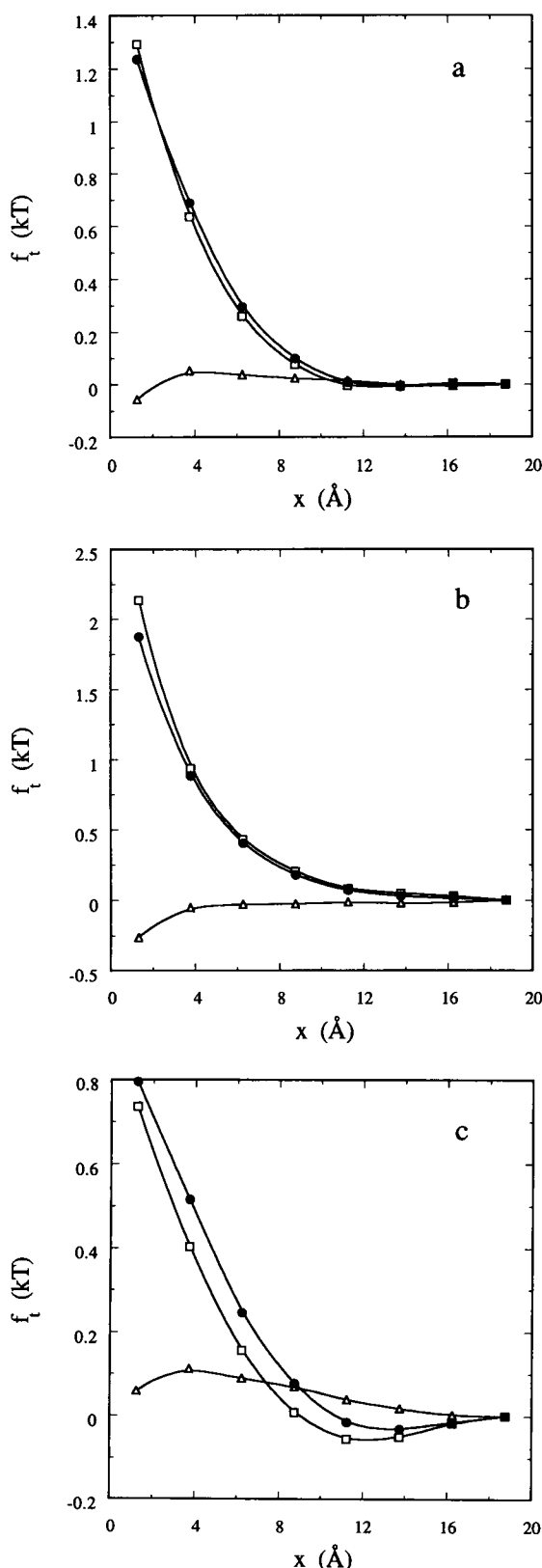


FIGURE 3 Chain free energy  $f_i$  (●) and its entropic,  $-Ts_i$  (□) and energetic,  $\epsilon_i$  (△) contributions, as a function of the distance from the protein wall, for  $C_{14}$  chains; relative to the unperturbed (asymptotic) value. In all three cases  $d_L^0 = 24.5 \text{ \AA}$ , corresponding to  $a_0 \approx 31.5 \text{ \AA}^2$ . The hydrophobic mismatch  $(d_p - d_L^0)/2$  is: 0 (a),  $+3.5 \text{ \AA}$  (b), and  $-3.5 \text{ \AA}$  (c). Note the different energy scales. The values of  $\xi$  (see text) for cases b and c are 3 and 6  $\text{\AA}$ , respectively.



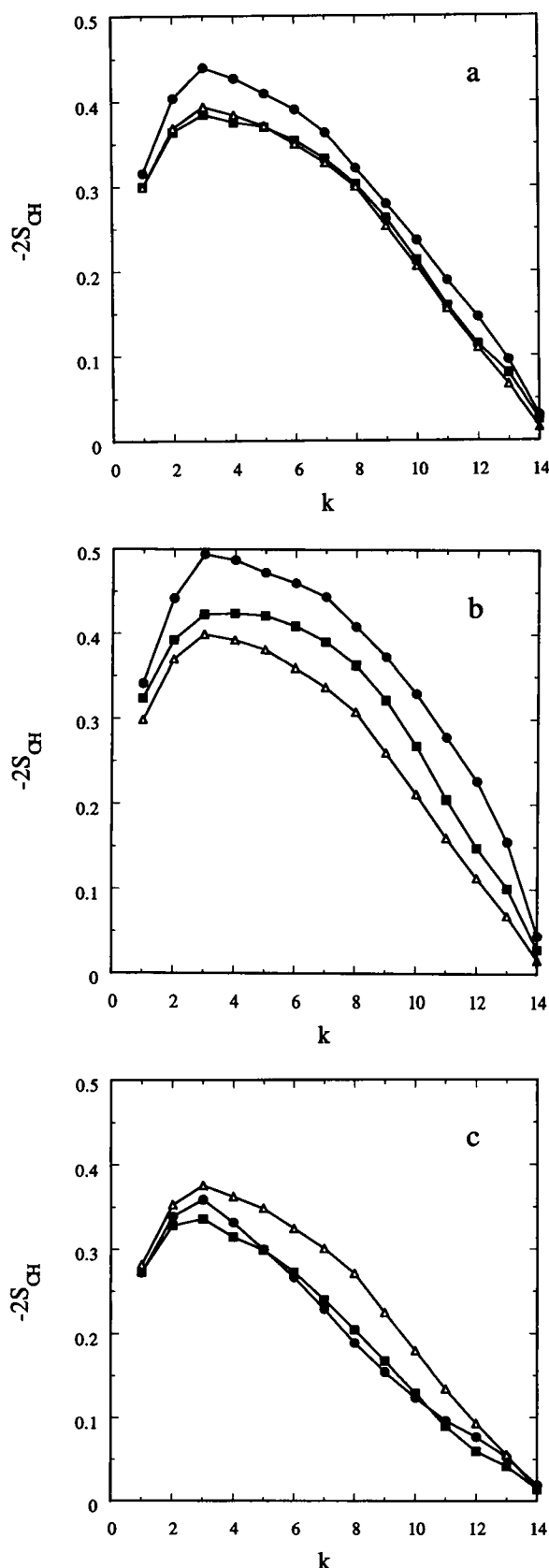


FIGURE 4 Orientational order parameter profiles of C—H bonds for chains originating at three different distances from the protein wall:  $x = 3.75$  Å (●),  $7.50$  Å (■), and  $18.75$  Å (△).  $k$  denote the carbon number along the  $C_{14}$  lipid chain.  $a$ ,  $b$ , and  $c$  correspond to  $(d_p - d_L^0)/2 = 0, +3.5$  and  $-3.5$  Å, respectively.  $d_L^0 = 24.5$  Å ( $a_0 = 31.5$  Å<sup>2</sup>).

originating from the interface at distance  $x$  from the protein. The membrane normal is parallel to the  $z$ -axis, Fig. 1. Recall that  $0 \leq -2S_k \leq 1$ ;  $S_k = -1/2$  for a fully stretched (“all-trans”) chain perpendicularly oriented with respect to the (asymptotic) interface, whereas  $S_k = 0$  for a random distribution of bond orientations. (The relatively low values of  $|S_k|$  for the first two bonds are due to the fact that in our calculations the corresponding  $CH_2$  segments are allowed to protrude slightly into the aqueous region; see Appendix).

In a pure membrane the bond order parameter profile, at a given temperature, depends only on the average cross sectional area per chain,  $a$ ; namely,  $\langle |S_k| \rangle$  increases monotonically as  $a$  decreases; for small values of  $a$ , i.e., a thick membrane, the chains must stretch out, resulting in high orientational ordering. Thus, if  $a(x) = a_0 = \text{constant}$ , as in the case  $d_p = d_L^0$ , Fig. 4 *a*, any deviation of  $S_k(x)$  from the asymptotic (unperturbed) value  $S_k(x = \infty)$ , is due to chain alignment induced by the presence of the protein wall. Furthermore, this effect is expected to be significant only for those chains originating at distance  $x < \sqrt{a_0}/2$  from the protein, as confirmed by the results in Fig. 4 *a*. The increase in  $|S_k|$  is expected to be larger for  $d_p > d_L^0$ , due to chain stretching ( $a(x) \leq a_0$ ), and to decrease gradually with  $x$  as  $a(x)$  approaches  $a_0$ , Fig. 4 *b*. The opposite behavior prevails when  $d_p < d_L^0$ , Fig. 4 *c*.

These trends are summarized in Fig. 5, which shows the average local bond order parameters  $\langle S_{CH} \rangle = (\sum_k S_k)/n$  as a function of the distance from the protein; the averaging includes the C—H bonds corresponding to carbons  $k = 1-14$  of the chains. (On the relationships between various bond order parameters see, e.g., Seelig and Seelig (1980) and Edholm (1987).) It should be noted, as previously observed by Marcelja (1976), that  $\langle S_{CH} \rangle$  is not a constant even if  $d_L(x) = d_p^0$ , i.e., in the case of perfect lipid-protein hydrophobic matching. In this case the average order parameter in the

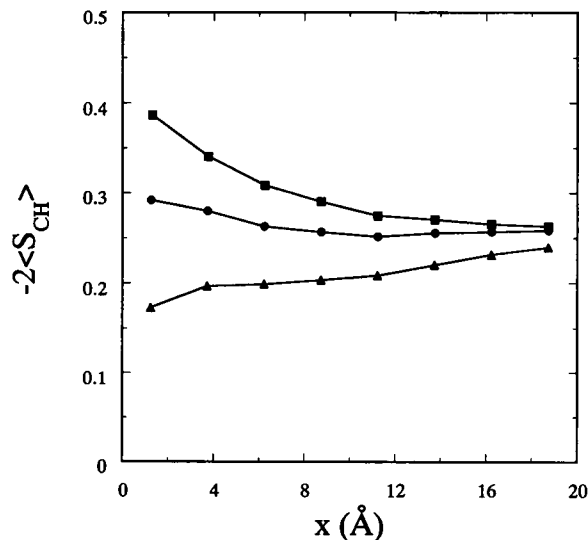


FIGURE 5 Average bond order parameters as a function of the distance from the protein, for the three cases considered in Fig. 4.  $(d_p - d_L^0)/2 = 0$  (●),  $+3.5$  Å (■), and  $-3.5$  Å (▲).

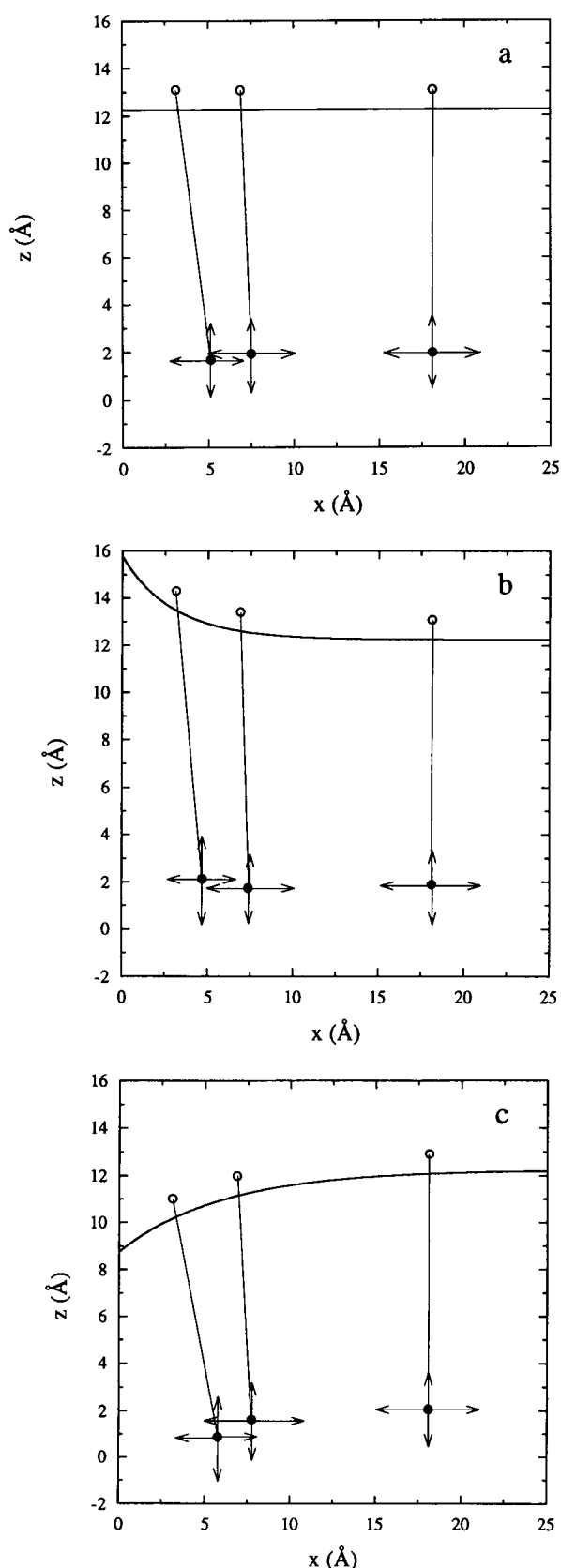


FIGURE 6 Schematic illustration of the hydrophobic interfacial profile and the effect of the protein wall on the average chain end-to-end vector. *a*, *b*, and *c* correspond to zero, positive (+3.5 Å) and negative (-3.5 Å) mismatch, for the same cases considered in Figs. 3–5. For each case the figure shows three representative head-group positions (symbolized by open

circles). The vertical, *z*, scale measures the distance from the bilayer's midplane. The average position of the terminal (CH<sub>3</sub>) group is symbolized by a solid circle. The lengths of the vertical and horizontal bars attached to the terminal group indicate the root-mean-square deviations along the *z* and *x* axes.

vicinity of the protein is (slightly) larger than the asymptotic value, due to the aligning effect of the rigid hydrophobic wall. Thus, one cannot expect a strictly linear (or some other simple) relationship between  $\langle S \rangle$  and  $d_L(x) - d_p$ .

The results shown in Figs. 4 and 5 are in good qualitative agreement with magnetic resonance measurements of the effects of hydrophobic solutes on orientational bond order parameters (Nezil and Bloom, 1992; Bloom et al., 1991). It should be noted however that <sup>2</sup>H NMR does not provide information on the local (i.e., *x*-dependent)  $S_k$  profiles but, rather, on their average over all positions *x* relative to the protein. The latter depend on the concentration of proteins in the membrane as well as on their shape (Jähnig et al., 1982; Nezil and Bloom, 1992).

As noted by Jähnig et al. (1982), the boundary conditions imposed by the protein on lipid chain order affect not only the bond order parameters but also induce a tilt of the “director,” i.e., of the average orientation of the chain axis relative to the membrane plane. The tilt angle  $\chi$  may be defined as the angle between the end-to-end vector (connecting the head-group P and the terminal chain segment CH<sub>3</sub>), and the *z*-axis. Clearly,  $\chi = \chi(x)$  decays to zero as *x* increases, as is illustrated in Fig. 6 for zero, positive and negative hydrophobic mismatches. Also shown are the root-mean-square deviations of the chain terminus in the *x* and *z* directions, e.g., the length of horizontal lines attached to the chain end is  $\sigma_n(x) = \langle (X_n - \langle X_n \rangle)^2 \rangle^{1/2}$  where the averaging is over all chain conformations  $\alpha$ , of a chain whose head-group is fixed at a given *x*. The tilt angle of chains originating at small *x* is due to repulsion by the wall, which is opposed by repulsions due to chains originating at  $x' > x$ . Interchain repulsion increases as the head-group density  $\sigma(x) \sim d_L(x)$  increases. Hence, it is expected that (for small *x*)  $\chi(x)$  will be relatively large for  $d_p < d_L(x)$  and small for  $d_p > d_L(x)$ , as confirmed by the results in Fig. 6. Note also, again as expected, that the average chain length is largest when  $d_p > d_L(x)$ , and that interdigitation between the two monolayers is apparent when  $d_p < d_L(x)$ .

## b) Adding interfacial contributions

From the above analysis it follows that  $\Delta F_t > 0$ , for all  $d_p - d_L^0$ , due primarily to the loss of conformational entropy (flexibility) experienced by the lipid chains in the protein's periphery. The chain deformation free energy is large when  $d_p - d_L^0 > 0$  and decreases gradually as the hydrophobic mismatch  $d_p - d_L^0$  decreases; (reaching a minimum value at some negative mismatch  $d_p - d_L^0 < 0$  where the average cross sectional area per chain  $\langle a \rangle \sim a_t > a_o$ , as discussed in section 2).

On the other hand, the interfacial term in the perturbation free energy,  $\Delta F_h = \int dx \sigma(x) [f_h(x) - f_h^0]$ , is large when  $d_p$

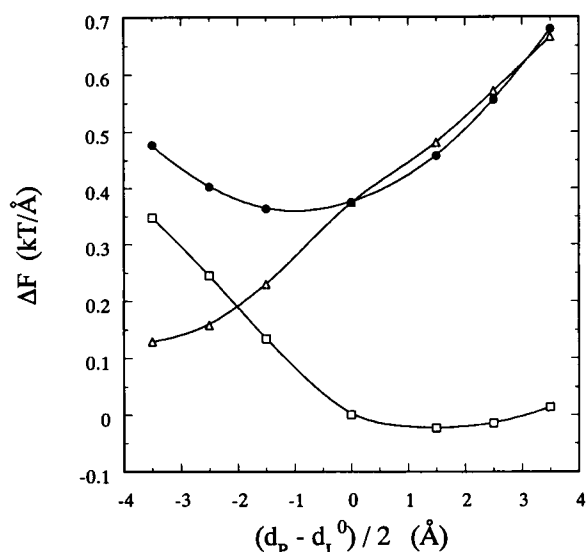


FIGURE 7 Tail ( $\Delta$ ), head ( $\square$ ), and total ( $\bullet$ ) deformation free energy (per unit length of protein perimeter) as a function of the lipid-protein hydrophobic mismatch. The membrane is composed of  $C_{14}$  lipid with head-group interaction parameters  $\gamma = 0.12 \text{ kT}/\text{\AA}^2$  and  $a_h = 20 \text{ \AA}^2$ ; the unperturbed bilayer thickness is  $d_L^0 = 24.5 \text{ \AA}$  ( $a_0 = 31.5 \text{ \AA}^2$ ). The plotted values of  $\Delta F$  correspond, for each mismatch, to the optimal value of the decay lengths  $\xi$ .

$< d_L^0$  and small when  $d_p > d_L^0$ . This is due to the hydrophobic (surface tension) contribution  $\gamma a(x)$  to  $f_h(x)$ , see Eq. 12, which decreases with the local thickness of the bilayer. Thus, since  $\Delta F_t$  and  $\Delta F_h$  display opposite dependencies on  $d_p - d_L^0$ , it is expected that  $\Delta F = \Delta F_t + \Delta F_h$  will obtain a minimum around  $d_p \approx d_L^0$ . For a given value of the hydrophobic mismatch,  $\Delta F$  depends on the coherence length  $\xi$ , cf. Eq. 1,

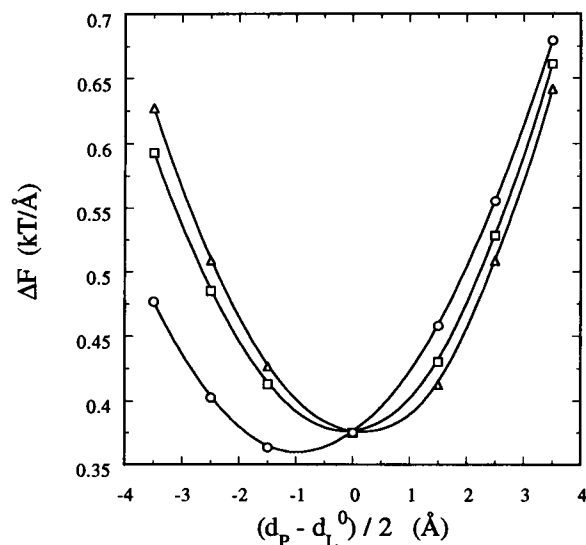


FIGURE 8 Lipid-protein interaction free energy (per unit protein length) as a function of the hydrophobic mismatch, for  $C_{14}$  chains. The three curves correspond to different choices of the head-group interaction parameter  $a_h$ ;  $a_h = 20 \text{ \AA}^2$  ( $\circ$ ),  $10 \text{ \AA}^2$  ( $\square$ ), and  $0$  ( $\Delta$ ). In all cases  $\gamma = 0.12 \text{ kT}/\text{\AA}^2$ . The optimal areas per head-group (of the unperturbed bilayer) are  $a_0 \approx 32 \text{ \AA}^2$  for all cases ( $d_L^0 = 24.5 \text{ \AA}$ ).

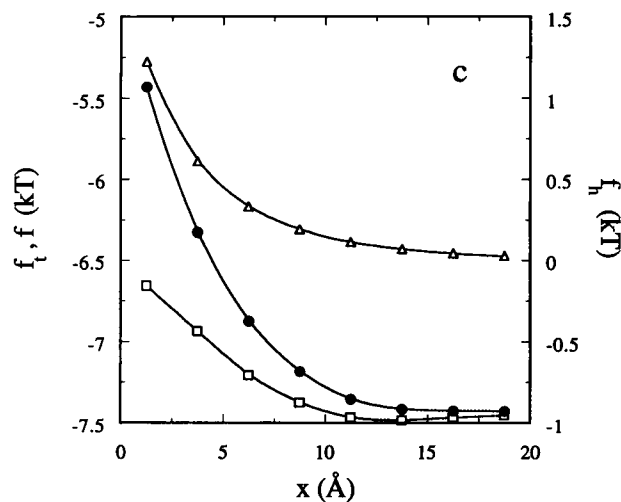
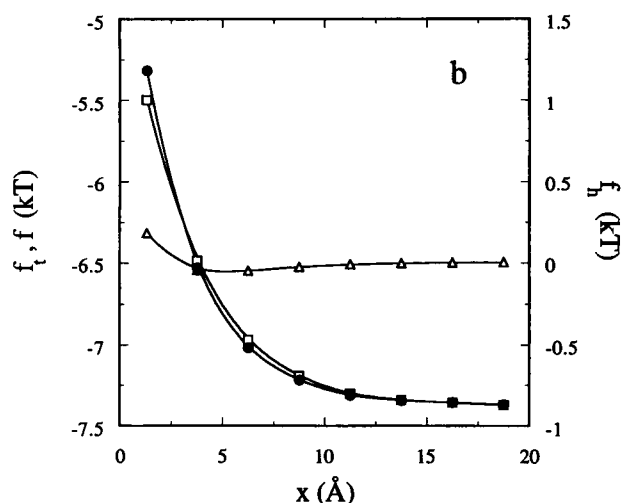
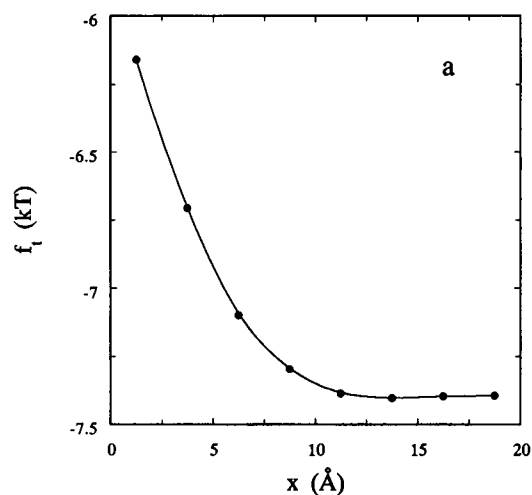


FIGURE 9 Tail ( $\square$ ) and head ( $\Delta$ ) contributions to the local free energy per molecule ( $\bullet$ ), as a function of the distance from the protein wall, relative scale. The results shown are for  $C_{14}$  chain with  $d_L^0 = 24.5 \text{ \AA}$ , ( $a_0 = 31.5 \text{ \AA}^2$ ),  $\gamma = 0.12 \text{ kT}/\text{\AA}^2$ , and  $a_h = 20 \text{ \AA}^2$ . a, b, and c correspond to  $(d_p - d_L^0)/2 = 0$  (constant head free energy),  $+3.5$  and  $-3.5 \text{ \AA}$ , respectively. Note the different energy scales (all relative).

which determines how  $d_L(x)$  varies with  $x$ . For every protein thickness,  $d_P$ , the bilayer will adjust  $\xi$  so as to minimize  $\Delta F$ .

The head and tail contributions to the deformation free energy, and their sum  $\Delta F = \Delta F_h + \Delta F_t$  (per unit length of the protein's circumference) are shown as a function of  $d_P - d_L^0$  in Fig. 7. The results correspond to interfacial head-group parameters  $\gamma = 0.12 \text{ kT}/\text{\AA}^2$  and  $a_h = 20 \text{ \AA}^2$ , for a bilayer composed of  $C_{14}$  chains with a hydrophobic thickness  $d_L^0 = 24.5 \text{ \AA}$ , corresponding to  $a_o \approx 32 \text{ \AA}^2$ . For each value of  $d_P - d_L^0$ ,  $\Delta F$  has been minimized with respect to  $\xi$ , yielding  $\xi \approx 6, 7, 7, 3, 3$ , and  $3 \text{ \AA}$ , for  $(d_P - d_L^0)/2 = -3.5, -2.5, -1.5, +1.5, +2.5$ , and  $+3.5 \text{ \AA}$ , respectively. Note that for the above choice of  $\gamma$  and  $a_h$  the minimal  $\Delta F$  is obtained for a slightly negative mismatch. For  $d_P - d_L^0 = 0$  we have used  $a(x) = a_o = \text{constant}$ , in accordance with Eq. 1. Yet it should be noted that the calculated value of  $\Delta F$  for this case could have been lower than that shown in Fig. 7 by allowing a variable  $a(x)$  (e.g.,  $a(x) \geq a_o$  for  $x \geq 0$  which would release some of the conformational strain, and then allowing  $a(x) \rightarrow a_o$  at larger  $x$ ). In Fig. 8 we show again  $\Delta F$  vs.  $d_P - d_L^0$  for the above case, as well as for two additional choices of the head-group repulsion parameter  $a_h$ ;  $a_h = 0$  and  $10 \text{ \AA}^2$ . In all three cases  $\gamma = 0.12 \text{ kT}/\text{\AA}^2$  and  $a_o \approx 32 \text{ \AA}^2$ ; recall from section 2 that  $a_o$  is not very sensitive to  $a_h$ , provided  $a_h$  is significantly smaller than  $a_o$  (see Fig. 2). As expected, weaker head-group repulsion, i.e., smaller  $a_h$ , enhances the hydrophobic free energy cost associated with increasing the membrane's interfacial area, resulting in larger  $\Delta F$  for  $d_P < d_L^0$  and smaller for  $d_P > d_L^0$ .

In Fig. 9 we show, for negative and positive hydrophobic mismatches, how the local free energies per molecules,  $f_h(x)$  and  $f_t(x)$ , vary with the distance from the protein. As noted already in Fig. 7, the head-group contribution is large and decreases rapidly with  $d_P - d_L^0$  when  $d_P < d_L^0$ , reaching a small, nearly constant, value for  $d_P \geq d_L^0$ .

Finally, we consider the  $\xi$  dependence of  $\Delta F(\xi) = \Delta F_t(\xi) + \Delta F_h(\xi)$ . Both  $\Delta F_t$  and  $\Delta F_h$  depend rather sensitively on  $\xi$  and vary in opposite manner, as illustrated in Fig. 10. For  $d_P < d_L^0$ ,  $\Delta F_t$  decreases with  $\xi$  since a larger number of chains benefit from the increased conformational freedom associated with packing at  $a > a_o$  ( $d_L < d_L^0$ ). On the other hand,  $\Delta F_h$  increases with  $\xi$  due to the larger surface area, and hence larger  $\gamma a$  contributions. The opposite behavior characterizes the system when  $d_P > d_L^0$ . The value of  $\xi$  at which  $\Delta F(\xi)$  obtains its minimum depends rather sensitively on the model parameters. For instance, for  $\gamma = 0.12 \text{ kT}/\text{\AA}^2$ ,  $a_h = 20 \text{ \AA}^2$  the minima corresponding to  $(d_P - d_L^0)/2 = +3.5$  and  $-3.5 \text{ \AA}$  are at  $\xi \approx 3 \text{ \AA}$  and  $6 \text{ \AA}$ , respectively, whereas for  $\gamma = 0.12 \text{ kT}/\text{\AA}^2$ ,  $a_h = 10 \text{ \AA}^2$ , the minimum of  $\Delta F$  for both the positive and the negative mismatch is at  $\xi \approx 5 \text{ \AA}$ . In all cases the range of the perturbation extends over very few molecular diameters.

#### 4. DISCUSSION

In the model described in the previous sections the lipid-protein interaction free energy has been treated as a sum of

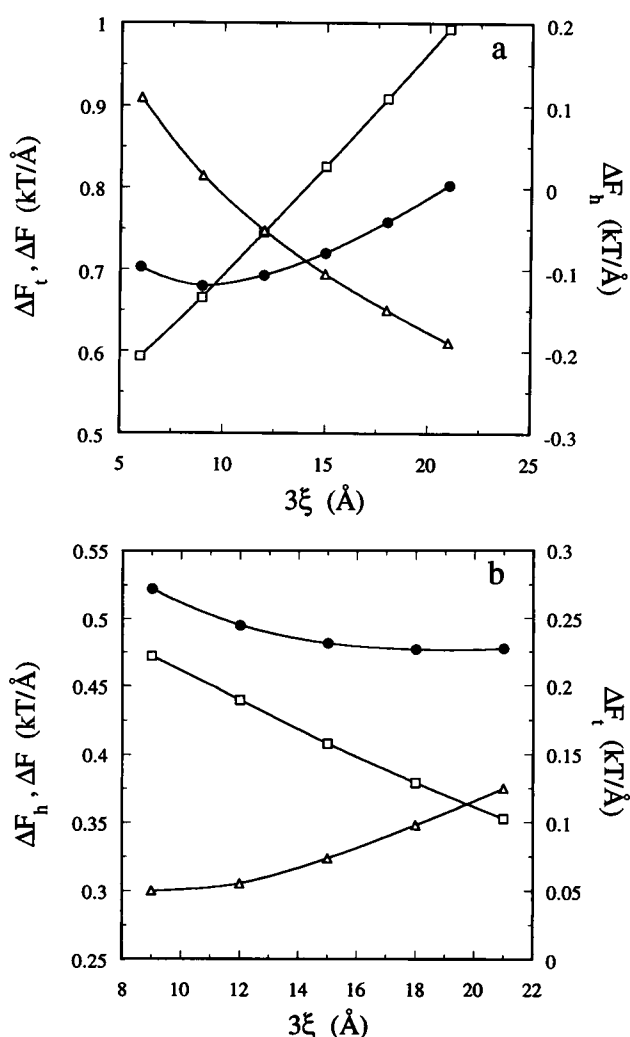


FIGURE 10 Tail ( $\square$ ), head ( $\Delta$ ), and total ( $\bullet$ ) deformation free energies (per unit protein circumference length) as a function of the coherence length  $\xi$ , for  $(d_P - d_L^0)/2 = +3.5 \text{ \AA}$  (a) and  $-3.5 \text{ \AA}$  (b). The results shown are for  $C_{14}$  chains,  $d_L^0 = 24.5 \text{ \AA}$ ,  $\gamma = 0.12 \text{ kT}/\text{\AA}^2$  and  $a_h = 20 \text{ \AA}^2$ . Note the different (relative) scales in the two cases. The (shallow) minimum in  $\Delta F$  in b is at  $3\xi \sim 18 \text{ \AA}$ .

a surface (or head-group region) term, and a chain (or hydrophobic core) term,  $\Delta F = \Delta F_h + \Delta F_t$ . The surface contribution accounts for changes in the hydrocarbon-water interfacial area associated with nonzero hydrophobic mismatch, and is largely due to the surface tension contribution (" $\gamma a$ "). It is large and positive when  $d_P < d_L^0$  and relatively small when  $d_P > d_L^0$ . The chain term,  $\Delta F_t$ , may be regarded as a sum of two, not strictly separable, contributions. One of these, which is always positive, even in the case of perfect hydrophobic matching ( $d_P = d_L^0$ ), involves the loss of conformational entropy imposed by the presence of the impenetrable protein wall. In fact, for  $d_P = d_L^0$  this is the only contribution to  $\Delta F$ , as noted already by Marcelja (1976). The other contribution to  $\Delta F_t$  is associated with the requirement for hydrophobic matching at the lipid-protein interface  $d_P = d_L(x=0)$ . For  $d_P > d_L^0$  this condition implies enhanced chain stretching, and thus larger  $\Delta F_t$  (as compared to the case

$d_p = d_L^0$ ), whereas  $d_p < d_L^0$  relieves part of the chain stretching energy, resulting in lower  $\Delta F_t$ . Since  $\Delta F_h$  is large for  $d_p < d_L^0$  and small for  $d_p > d_L^0$ , while  $\Delta F_t$  displays an opposite behavior  $\Delta F$  is generally minimal around  $d_p = d_L^0$ .

The chain contributions to  $\Delta F$  have been treated in considerable detail. On the other hand, for the surface terms, especially for the highly specific head-group repulsive contribution, we have used an approximate phenomenological representation. Our model has involved various other approximations and assumptions. For instance, it was assumed that the cohesive, van der Waals, attraction between lipid chains is the same as that between lipid chains and the (hydrophobic region of the) protein. Similarly, our model did not account for the interactions between lipid and protein hydrophilic groups, since these depend on the specific nature of these groups. Nevertheless, we believe that the model analyzed in the previous sections captures many of the essential mechanisms responsible for lipid-protein interaction. With the above reservations in mind we turn now to a brief comparison of our model with two alternative approaches for the calculation of  $\Delta F$ , and then to a brief discussion of the possible extensions of the model.

In the mattress model (Mouritsen and Bloom, 1984; Mouritsen and Bloom, 1993) mentioned in section 1 the interfacial profile of the membrane hydrophobic core is approximated by a step function, namely,  $d_L(x) = d_L^0 = \text{constant}$ , corresponding formally to  $\xi = 0$  in Eq. 1. Following this picture, the lipid-protein interaction free energy (per unit length of the protein circumference) is expressed in the form  $\Delta F = \eta |d_p - d_L^0| + \nu \min\{d_p, d_L^0\}$ . The first term in this expression accounts for the excess hydrophobic free energy associated with exposing the lipid chains (when  $d_L^0 > d_p$ ) or the protein (when  $d_L^0 < d_p$ ) to the surrounding aqueous solution. Accordingly,  $\eta$  is interpreted as an effective surface tension which is assumed to be about twice as large ( $\eta = 2\epsilon$ ) for lipid-water contact as compared to protein-water contact ( $\eta = \epsilon$ ). The second term, which is proportional to the contact area between the lipid chains and the hydrophobic region of the protein, is interpreted as the excess van der Waals lipid-protein interaction (relative to the average of lipid-lipid and protein-protein interaction);  $\nu$  is positive and is larger when the lipid membrane is in the "fluid" state as compared to the ordered ("gel") state, (the mattress model yields good agreement with experiment for  $\nu_f \sim 5\nu_g$ ). In its full version the mattress model includes also an elastic deformation term, of the form  $\sim (d_p - d_L^0)^2$ , which is assumed to be negligible at low protein concentrations. The model parameters are determined by fitting its predictions to experimental data concerning the dependence of the membrane gel-fluid transition temperature on protein concentration.

The molecular picture underlying the mattress model is obviously quite different from ours. Nevertheless, some of the trends predicted by the two models are rather similar. For instance, both models predict  $\Delta F > 0$  for  $d_p = d_L^0$ . Yet, in the mattress model this is attributed to the excess van der Waals energy  $\Delta F = \nu d_p = \nu d_L^0 > 0$ , whereas in our model the relevant contribution is the loss of chain conformational

entropy. In fact, for the case  $d_L^0 = d_p$ , we have performed additional calculations (not reported in section 3) for lipids of different chain length  $n$  ( $n = 12, 14, 16$ ), and found that for any given area per chain  $a$ ,  $\Delta F$  increases nearly linearly with  $n$  and hence with  $d_L^0$  ( $= 2n\nu/a$ ), consistent with the mattress model. Furthermore, the same calculations reveal a strong increase of  $\Delta F$  with  $a$ , i.e., with the degree of chain disorder (or "fluidity"), which is consistent with  $\nu_f > \nu_g$ .

When  $d_p \neq d_L^0$  the mattress model includes the additional term  $\eta |d_L^0 - d_p|$ . In our model the hydrophobic mismatch results in two additional contributions, the sum of which is generally positive. Namely, the enhanced (reduced) chain stretching when  $d_p > d_L^0$  ( $d_p < d_L^0$ ), and the change in surface energy which is low for  $d_p > d_L^0$  and large and positive when  $d_p < d_L^0$ . The mattress model does not explicitly account for chain flexibility effects. However, in our opinion, the parameter  $\eta$  could (and in view of its low numerical value as compared to the bare tension  $\gamma$  also should) be interpreted as an effective surface tension, representing the balance between the positive lateral chain pressure ( $-\partial f_c/\partial a > 0$ ) and the negative ( $-\gamma$ ) surface pressure (see section 1 and Hladky and Gruen, 1982).

Finally, since the parameters in the mattress model have been determined by comparison to experimental data on the fluid-gel transition, whereas our calculations have been restricted to the fluid membrane state a detailed quantitative comparison between the two models is not warranted at this stage. Nevertheless, if the mattress model is used to estimate changes in  $\Delta F$  for, say, different values of  $d_p - d_L^0$  for a given  $d_L^0$ , one obtains typically  $\delta(\Delta F) \sim 0.1kT/\text{\AA}$  which is of the same order of magnitude of  $\delta(\Delta F)$  values obtained in our calculations, see Fig. 8.

Several authors have calculated the (protein induced) lipid deformation free energy based on the continuum theory of elastic deformations in liquid crystals (Huang, 1986; Helfrich and Jakobsson, 1990). The theory has been applied to study the changes in  $\Delta F$  associated with gramicidin dimerization in lipid membranes; the quantity calculated is  $\delta(\Delta F) = \Delta F_d - 2\Delta F_m$ , where  $\Delta F_d$  and  $\Delta F_m$  are the lipid deformation free energies induced by the dimer and the monomer, respectively. It is tacitly assumed that the monomers do not affect the bilayer thickness and hence  $\Delta F_m = 0$ , whereas dimer formation imposes a negative hydrophobic mismatch, i.e.,  $d_p = d_L(x=0) < d_L^0$ . In these continuum theories the deformation free energy is expressed as a sum of splay, compression and surface tension terms and the relevant elastic constants are taken from experimental data for pure (protein free) lipid membranes. The splay term accounts for changes in the local director (i.e., in the average lipid chain tilt angle), the compression involves changes in the membrane thickness and the (effective) surface tension accounts for changes in the interfacial area.

The applicability of a continuum elastic theory for calculating lipid-protein interaction is limited due to several factors. Among these are the short length scale (few molecular diameters) of the perturbation, and the conformational flexibility of the lipid chains which strongly couples

the splay (or bending) and compression deformations. It should also be noted that the surface tension used is not the bare hydrocarbon-water tension but, rather, the residual tension accompanying curvature deformations. Furthermore, since the elastic constants are those of the unperturbed bilayer, they do not explicitly account for the loss of conformational entropy implied by the presence of the rigid protein wall. On the other hand, these continuum models do not postulate a given interfacial profile (such as Eq. 1) but, rather, determine its form by a numerical variational procedure. An interesting outcome of the calculations is that the initial slope of the interfacial profile,  $(d[d_L(x)]/dx \text{ at } x = 0)$ , is negative even if  $d_L^0 > d_p$ . (A similar conclusion has recently been arrived at by another approach, involving polymer scaling considerations (Dan et al., manuscript submitted for publication).) This effect is mainly due to a lower splay deformation (as compared to  $d[d_L(x)]/dx \geq 0$ ), and it would be interesting to test it using our molecular approach. The numerical values predicted for  $\delta(\Delta F) = \Delta F_d$  (for  $d_L^0 - d_p \sim 7$  Å and  $d_L^0 \approx 22$  Å) are  $\sim(0.02\text{--}0.1)kT/\text{Å}$ , depending on the initial slope of the interfacial profile. These values are lower than those calculated by our approach, see Fig. 8. Recall, however, that in these models  $\Delta F_m = 0$ , whereas our model implies  $\Delta F_m > 0$ . In fact, assuming that the monomer, whose thickness is smaller than  $d_L^0/2$ , is attached to one of the interfaces, we expect two positive contributions to  $\Delta F_m$ . The first involves the loss of conformational entropy of the lipids surrounding the monomer, and the second involves the enhanced chain stretching of lipid chains originating at the opposite interface.

Although throughout this paper we have referred to lipid deformations induced by hydrophobic, transmembrane proteins, it is clear that the model described can be applied to any hydrophobic solute, e.g., cholesterol molecules. Furthermore, the calculations can be extended to lipid mixtures as well as to an arbitrary shape and size of the hydrophobic solute. Similarly, the model can be applied to calculate solute-solute interactions, e.g., the lipid mediated protein-protein interaction (Marcelja, 1976; Abney and Owicki, 1985). We reiterate, however, that the most important elaboration of our approach, which is required to enhance its quantitative character, would be a more detailed treatment of the interactions governing the interfacial region. At least for some special systems of interest, this should be a feasible task.

## APPENDIX: THE NUMERICAL EVALUATION OF $P(\alpha; X)$

To calculate the Lagrange multipliers  $\lambda(X, Z; x)$  appearing in  $P(\alpha; x)$  we first divide the  $X, Z$  plane of the hydrophobic core into small elements  $\delta X \delta Z$ ; we typically use  $\delta X \approx \delta Z \approx 2.5$  Å. The range of  $X$  considered is  $0 \leq X \leq x_{\max}$  with  $x_{\max} = 25$  Å in most calculations. The range of  $Z = Z(x)$  is dictated by the shape of the hydrophobic core, i.e.,  $-d_L(x)/2 \leq Z(x) \leq d_L(x)/2$ . Then, within each  $\delta x$  interval we (randomly) choose two head-group positions  $x_h$ , and for each  $x_h$  generate many chain conformations  $\alpha = z_h, \Omega, b$ . More specifically, for every  $x_h$  we sample two  $z_h$  values for each of the two interfaces, such that  $d_L(x)/2 \leq |z_h(x)| \leq d_L(x)/2 + \Delta z$  with  $\Delta z \approx 1.8$  Å. For each head-group position  $x_h, z_h$  we generate all the possible (*trans*/

*gauche*) bond sequences,  $b$ , according to the rotational isomeric state model, discarding all non self-avoiding conformations. Then for each  $b$  we randomly choose nine overall chain orientations  $\Omega$ , with  $\Omega$  defined by the three Eulerian angles of the  $b$  chain. A considerable fraction of the  $\alpha$  values are classified as forbidden conformation and are discarded. These include all conformations which have one or more chain segment in the  $x < 0$  regime, i.e., inside the protein region. (Clearly, this implies considerable entropy loss for chains originating in the vicinity of the protein). Similarly, a conformation  $\alpha$  is forbidden if any of the carbons,  $k = 3 - n$  ( $n = 14$ ), protrudes beyond the hydrophobic core. Only the first and second  $\text{CH}_2$  groups along the chain are allowed to be outside the core, within the "roughness region"  $\Delta z$  specified above. Note however that the statistical weight of these "protruding" conformations is small, due to the requirement of uniform segment density inside the core. On the average, about "one-half" chain segment is found in the aqueous region.

All the allowed conformations contribute to  $\psi(X, Y, \alpha; x = x_h)$  which appear in Eq. 7. By summing over all head-group positions  $x_h$ , each weighted by  $\sigma(x = x_h)$ , as well as over all chain conformations  $\alpha$ , and using Eq. 8 for  $P(\alpha, x)$  we obtain an equation expressing the constraint of uniform, liquid-like, density in box  $\delta X \delta Z$  of the hydrophobic core. Repeating this procedure for all boxes  $\delta X \delta Z$  we obtain a set of  $M$  nonlinear equations for the  $M$  Lagrange multipliers  $\lambda(X, Z)$ ;  $M$  being the number of boxes. (For a symmetrical bilayer there are only  $M/2$ -independent  $\lambda$  values). These equations can be solved numerically, yielding all the *pdf* values  $P(\alpha; x)$  as given in Eq. 8.

Note that for chains originating at  $x \leq x_{\max}$  there will be many conformations in which one or more chain segments protrude into the region  $x > x_{\max}$ . Clearly, these are allowed conformations. By "mirror imaging" these conformations across the  $x_{\max}$  plane, we also take into account the contribution of chain conformations originating at  $x > x_{\max}$  to the segment densities in the  $x < x_{\max}$  region.

Once the *pdfs*  $P(\alpha; x)$  are known we can calculate any desirable chain conformational property, e.g., bond order parameter profiles, chain segment distributions, tilt angles, etc. Similarly, using Eq. 4 or Eq. 5 we can calculate local, or total, chain free energies, energies and entropies—all in the mean-field approximation, since these equations involve only singlet *pdf* values.

We thank Professor Erich Sackmann for many fruitful discussions. The Yeshaya Horowitz Association and The National Science Foundation administered by the Israel Academy of Science and Humanities are acknowledged for financial support.

The Fritz Haber Research Center is supported by the Minerva Gesellschaft für die Forschung, mbH, Munich, Germany. This work has been completed while one of the authors (A. Ben-Shaul) has been a Fellow at the Institute of Advanced Studies of The Hebrew University, Jerusalem.

## REFERENCES

- Abney, J. R., and J. C. Owicki. 1985. Theories of protein-lipid and protein-protein interactions in membranes. In: *Progress in Protein-Lipid Interactions*. A. Watts and J. J. H. M. de Pont, editors. Elsevier, Amsterdam. 1-60.
- Andelman, D. 1994. Electrostatic properties of membranes. In: *Membranes: Their Structure and Conformations*. Elsevier, Amsterdam. In press.
- Ben-Shaul, A., and W. M. Gelbart. 1993. Statistical thermodynamics of amphiphile self-assembly: structure and phase transitions in micellar solutions. In: *Micelles, Monolayers, Microemulsions and Membranes*. W. M. Gelbart, D. Roux, and A. Ben-Shaul editors. Springer, New York. Chap. 1. 1-104.
- Ben-Shaul, A., I. Szleifer, and W. M. Gelbart. 1985. Chain organization and thermodynamics in micelles and bilayers. *J. Chem. Phys.* 83:3597-3611.
- Bloom, M., E. Evans, and O. G. Mouritsen. 1991. Physical properties of the fluid lipid-bilayer component of cell membranes: a perspective. *Q. Rev. Biophys.* 24:293-397.
- Caille, A., D. Pink, F. De Verteuil, and M. J. Zuckermann. 1980. Theoretical models for quasi-dimensional mesomorphic monolayers and membrane bilayers. *Can. J. Phys.* 58:581-611.
- Dill, K. A., J. Naghizadeh, and J. A. Marqusee. 1988. Chain molecules at

- high densities at interfaces. *Annu. Rev. Phys. Chem.* 39:425–462.
- Dill, K. A., and D. Stigter. 1988. Lateral interactions among phosphatidylcholine and phosphatidylethanolamine head groups in phospholipid monolayers and bilayers. *Biochemistry*. 27:3446–3453.
- Edholm, O. 1982. Order parameters in hydrocarbon chains. *Chem. Phys.* 65:259–270.
- Edholm, O., and J. Johansson. 1987. Lipid bilayer polypeptide interactions studied by molecular dynamics simulation. *Eur. Biophys. J.* 14:203–209.
- Elliott, J. R., D. Needham, J. P. Dilger, and D. A. Haydon. 1983. The effects of bilayer thickness and tension on gramicidin single-channel lifetime. *Biochim. Biophys. Acta.* 735:95–103.
- Ennis, J. 1992. Spontaneous curvature of surfactant films. *J. Chem. Phys.* 97:663–678.
- Flory, P. J. 1969. *Statistical Mechanics of Chain Molecules*. Wiley-Interscience, New York.
- Gruen, D. W. R. 1985a. A model for the chains in amphiphilic aggregates. I: Comparison with a molecular dynamics simulation of a bilayer. *J. Phys. Chem.* 89:146–153.
- Gruen, D. W. R. 1985b. The standard picture of ionic micelles. *Prog. Colloid Polymer Sci.* 70:6–16.
- Helfrich, P., and E. Jakobsson. 1990. Calculation of deformation energies and conformations in lipid membranes containing gramicidin channels. *Biophys. J.* 57:1075–1084.
- Hladky, S. B., and D. W. R. Gruen. 1982. Thickness fluctuations in black lipid membranes. *Biophys. J.* 38:251–258.
- Hladky, S. B., and D. A. Haydon. 1984. Ion Movements in gramicidin channels. In: *Current Topics in Membranes and Transport*. Vol. 21. Ion Channels: Molecular and Physiological Aspects. F. Bronner and W. D. Stein, editors. Academic Press, New York. 327–372.
- Huang, H. W. 1986. Deformation free energy of bilayer membrane and its effect on gramicidin channel lifetime. *Biophys. J.* 50:1061–1070.
- Israelachvili, J. N. 1985. *Intermolecular and Surface Forces*. Academic Press, London.
- Israelachvili, J. N., D. J. Mitchell, and B. W. Ninham. 1976. Theory of self-assembly of hydrocarbon amphiphiles into micelles and bilayers. *J. Chem. Soc. Faraday Trans. II.* 72:1525–1568.
- Jähnig, F. 1981. Critical effects from lipid-protein interaction in membranes. *Biophys. J.* 36:329–345.
- Jähnig, F., H. Vogel, and L. Best. 1982. Unifying description of the effect of membrane proteins on lipid order. Verification for the melittin/Dimyristoylphosphatidylcholine system. *Biochemistry*. 21:6790–6798.
- Kurrie, A., P. Rieber, and E. Sackmann. 1990. Reconstitution of transferrin receptor in mixed lipid vesicles. An example of the role of elastic and electrostatic forces for protein/lipid assembly. *Biochemistry*. 29:8274–8282.
- Lewis, B. A., and D. M. Engelman. 1983. Lipid bilayer thickness varies linearly with acyl chain length in fluid phosphatidylcholine vesicles. *J. Mol. Biol.* 166:211–217.
- Marcelja, S. 1976. Lipid-mediated protein interaction in membranes. *Biochim. Biophys. Acta.* 455:1–7.
- Mouritsen, O. G., and M. Bloom. 1984. Mattress model of lipid-protein interactions in membranes. *Biophys. J.* 46:141–153.
- Mouritsen, O. G., and M. Bloom. 1993. Models of lipid-protein interactions in membranes. *Annu. Rev. Biophys. Biomol. Struct.* 22:145–171.
- Nagle, J. F., and M. C. Wiener. 1988. Structure of fully hydrated bilayer dispersions. *Biochim. Biophys. Acta.* 942:1–10.
- Nagle, J. F., and D. A. Wilkinson. 1978. Lecitin bilayers, density measurements and molecular interactions. *Biophys. J.* 23:159–175.
- Nezil, F. A., and M. Bloom. 1992. Combined influence of cholesterol and synthetic amphiphilic peptides upon bilayer thickness in model membranes. *Biophys. J.* 61:1176–1183.
- Ott, A., W. Urbach, D. Langevin, R. Ober, and M. Waks. 1990. Light scattering study of surfactant multilayers elasticity. Role of incorporated proteins. *Eur. Lett.* 12:395–400.
- Owicki, J. C., and H. M. McConnell. 1979. Theory of protein-lipid and protein-protein interactions in bilayer membranes. *Proc. Natl. Acad. Sci. USA.* 76:4750–4754.
- Owicki, J. C., M. W. Springgate, and H. M. McConnell. 1978. Theoretical study of protein-lipid interactions in bilayer membranes. *Proc. Natl. Acad. Sci. USA.* 75:1616–1619.
- Pearson, L. T., S. I. Chan, B. A. Lewis, and D. M. Engelman. 1983. Pair distribution functions of bacteriorhodopsin and rhodopsin in model bilayers. *Biophys. J.* 43:167–174.
- Peschke, J., J. Riegler, and H. Möhwald. 1987. Quantitative analysis of membrane distortions induced by mismatch of protein and lipid hydrophobic thickness. *Biophys. J.* 14:385–391.
- Pink, D. A., and D. Chapman. 1979. Protein-lipid interactions in bilayer membranes: a lattice model. *Proc. Natl. Acad. Sci. USA.* 76:1542–1546.
- Riegler, J., and H. Möhwald. 1986. Elastic interactions of photosynthetic reaction center proteins affecting phase transitions and protein distributions. *Biophys. J.* 49:1111–1118.
- Ring, A. 1992. Influence of ion occupancy and membrane deformation on gramicidin A channel stability in lipid membranes. *Biophys. J.* 61:1306–1315.
- Sackmann, E. 1984. Physical basis of trigger processes and membrane structures. In: *Biological Membranes*. Vol. 5. Chap. 3. D. Chapman, editor. Academic Press, New York. 105–143.
- Scott, H. L., and S. L. Cherng. 1978. Monte Carlo studies of phospholipid lamellae. Effects of proteins, cholesterol, bilayer curvature, and lateral mobility on order parameters. *Biochim. Biophys. Acta.* 510:209–215.
- Scott, H. L., and T. J. Coe. 1983. A theoretical study of lipid-protein interactions in bilayers. *Biophys. J.* 42:219–224.
- Seelig, J., and A. Seelig. 1980. Lipid conformation in model membranes and biological membranes. *Q. Rev. Biophys.* 13:19–61.
- Small, D. M. 1986. *The Physical Chemistry of Lipids*. Plenum Publishing Corp., New York.
- Sperotto, M. M., and O. G. Mouritsen. 1988. Dependence of lipid membrane phase transition temperature on the mismatch of protein and lipid hydrophobic thickness. *Eur. Biophys. J.* 16:1–10.
- Sperotto, M. M., and O. G. Mouritsen. 1991. Mean-field and Monte Carlo simulation studies of the lateral distribution of proteins in membranes. *Eur. Biophys. J.* 19:157–168.
- Steinhuizen, L., D. Kramer, and A. Ben-Shaul. 1991. Statistical thermodynamics of molecular organization in the inverse hexagonal phases of amphiphiles. *J. Phys. Chem.* 95:7477–7483.
- Stigter, D., and K. A. Dill. 1988. Lateral interactions among phospholipid head groups at the heptane/water interface. *Langmuir*. 4:200–209.
- Szleifer, I., A. Ben-Shaul, and W. M. Gelbart. 1986. Chain statistics in micelles and bilayers: effects of surface roughness and internal energy. *J. Chem. Phys.* 85:5345–5358.
- Szleifer, I., A. Ben-Shaul, and W. M. Gelbart. 1987. Statistical thermodynamics of molecular organization in mixed micelles and bilayers. *J. Chem. Phys.* 86:7094–7109.
- Szleifer, I., D. Kramer, A. Ben-Shaul, W. M. Gelbart, and S. A. Safran. 1990. Molecular theory of curvature elasticity in surfactant films. *J. Chem. Phys.* 92:6800–6817.
- Tanford, C. 1980. *The Hydrophobic Effect*, Ed. 2. Wiley-Interscience, New York.
- Wennerström, H., and B. Lindman. 1979. Micelles, physical chemistry of surfactant association. *Phys. Rep.* 52:1–86.
- Wiener, M. C., and S. H. White. 1992. Structure of a fluid dioleoylphosphatidylcholine bilayer determined by joint refinement of x-ray and neutron diffraction data. II. Distribution and packing of terminal methyl groups. *Biophys. J.* 61:428–433.
- Wilkinson, D. A., and J. F. Nagle. 1981. Dilatometry and calorimetry of saturated phosphatidylethanolamine dispersions. *Biochemistry*. 20:187–192.
- Winterhalter, M., and W. Helfrich. 1992. Bending elasticity of electrically charged bilayers: coupled monolayers, neutral surfaces, and balancing stresses. *J. Phys. Chem.* 96:327–330.
- Zhang, Y., R. N. A. H. Lewis, R. S. Hodges, and R. N. McElhaney. 1992. Interaction of a peptide model of a hydrophobic transmembrane  $\alpha$ -helical segment of a membrane protein with phosphatidylcholine bilayers: differential scanning calorimetric and FTIR spectroscopic studies. *Biochemistry*. 31:11579–11588.